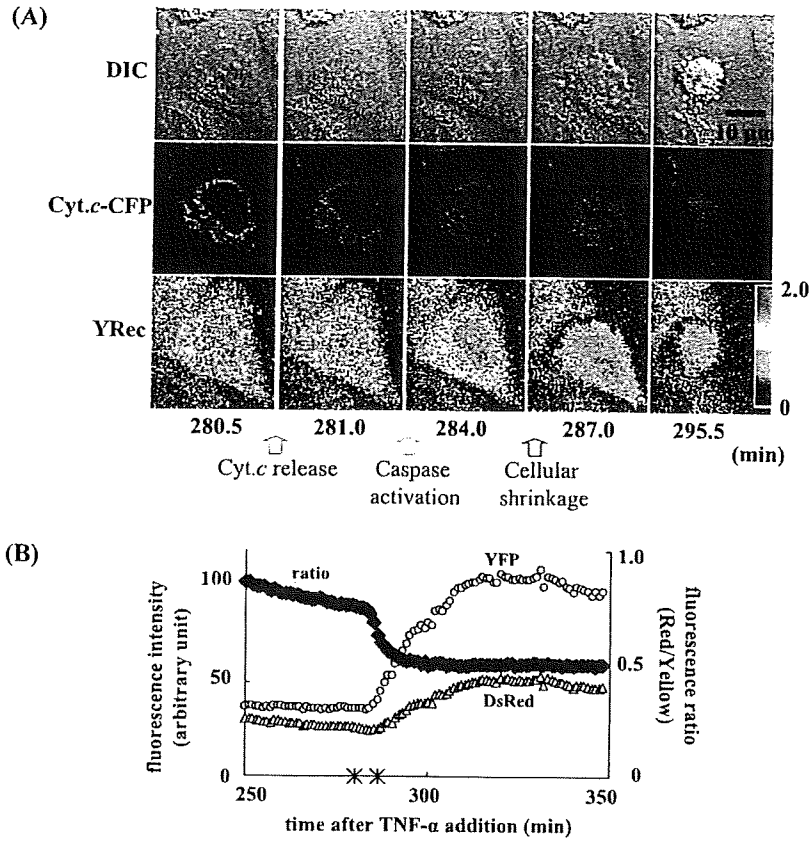

Fig. 1. Cyt.*c*-CFP release and caspase activation were monitored simultaneously in the same cells. A: DIC (upper), images showing the fluorescence of CFP (middle) and the fluorescence ratio of DsRed and YFP (DsRed /YFP, lower) during cell death are shown in pseudocolor. CFP and DsRed/YFP indicate the localization of cyt.*c*-CFP and caspase activation, respectively. B: Changes in YRec fluorescence in the cell shown in panel A were plotted. YFP and DsRed are shown with their fluorescence ratios. The asterisks indicate time points at which cyt.*c*-CFP were released and cell shrinkage was observed. The horizontal axis represents the point in time after the addition of TNF-*α*.

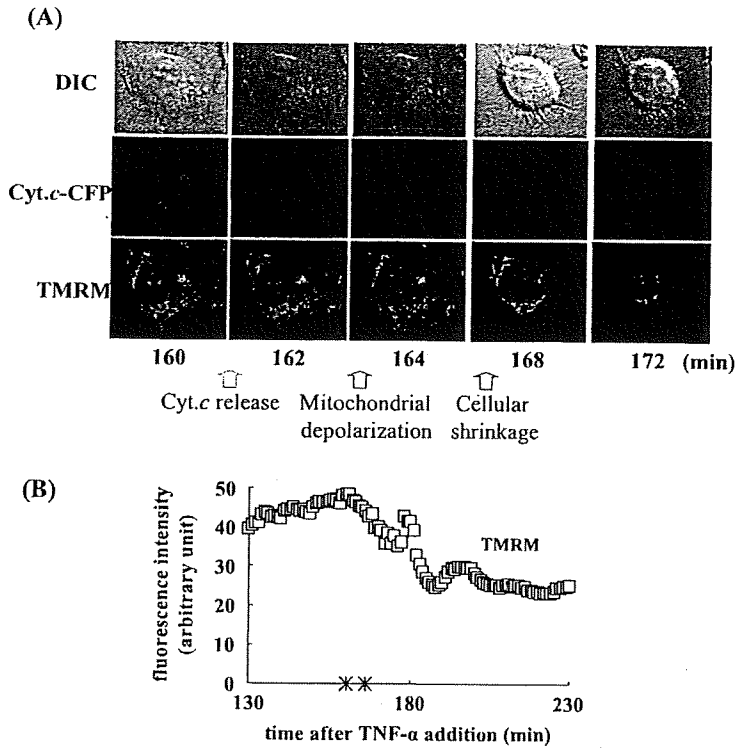

Fig. 2. Cyt.*c*-CFP release and mitochondrial depolarization were monitored simultaneously in the same cell. A: DIC (upper), images showing the fluorescence of CFP (middle) and the fluorescence of TMRM (lower) during cell death are shown in pseudocolor. CFP and TMRM fluorescence indicate the localization of cyt.*c*-CFP and the mitochondrial membrane potential, respectively. B: Changes in TMRM fluorescence of the cells in panel A during cell death were plotted. The asterisks indicate time points at which cyt.*c*-CFP were released and cell shrinkage was observed. The horizontal axis represents the point in time after the addition of TNF-*α*.

observed after this time point was unexpected, but is thought to have been the result of cellular shrinkage. Because the cell volume was reduced, the DsRed became concentrated, and the fluorescence increased. The reduction in the fluorescence ratio clearly indicated a reduction in FRET, which indicated both the cleavage of YRec as well as caspase activation. The asterisks indicate the time point of cyt.*c*-CFP release and cellular shrinkage, as determined based on the results shown in Fig. 1A. In this cell, cyt.*c*-CFP was released 280.5 min after the addition of TNF-α, and caspase activation was initiated 3 min after cyt.*c*-CFP release; the cell then started to shrink 3 min after caspase activation. Cyt.*c*-CFP release, caspase activation, and cellular shrinkage were observed in this order in all of the dying cells examined.

Simultaneous imaging of cyt.c-CFP and TMRM

HeLa cells expressing cyt.*c*-CFP were treated with TMRM and TNF-α. Delocalization of cyt.*c*-CFP and mitochondrial depolarization were observed with a resolution period of 1 min. All dying cells exhibited cyt.*c*-CFP release, mitochondrial depolarization, and shrinkage of the cell body. Figure 2A shows a typical fluorescent image of a dying cell. In this cell, cyt.*c*-CFP was released at 161 min, and cell shrinkage began at 167 min after the addition of TNF-α. Changes in TMRM fluorescence are plotted in Fig. 2B. TMRM fluorescence started to decrease at 164 min, thus indicating that the mitochondria started to depolarize at this point in time.

In a comparison of the starting points of these three events, it was found that the release of cyt.*c*-CFP always preceded mitochondrial depolarization and cellular shrinkage. Mitochondrial depolarization was observed earlier than cellular shrinkage in this particular cell, but was observed later in other cells. The temporal order of the timing of the initiation of mitochondrial depolarization and cellular shrinkage was not consistent. Mitochondrial depolarization preceded cellular shrinkage in 4 of the 10 cells, and cellular shrinkage preceded mitochondrial depolarization in 6 of the cells observed here.

Temporal relationships between mitochondrial changes, caspase activation, and cellular shrinkage

We observed 10 – 22 cells in each of these experiments, the results of which are shown in Figs. 1 and 2. We then determined the timing of cyt.*c* release, cellular shrinkage, and mitochondrial depolarization, or caspase activation in each cell. To clarify the temporal relationships between these cellular events, relative timing was

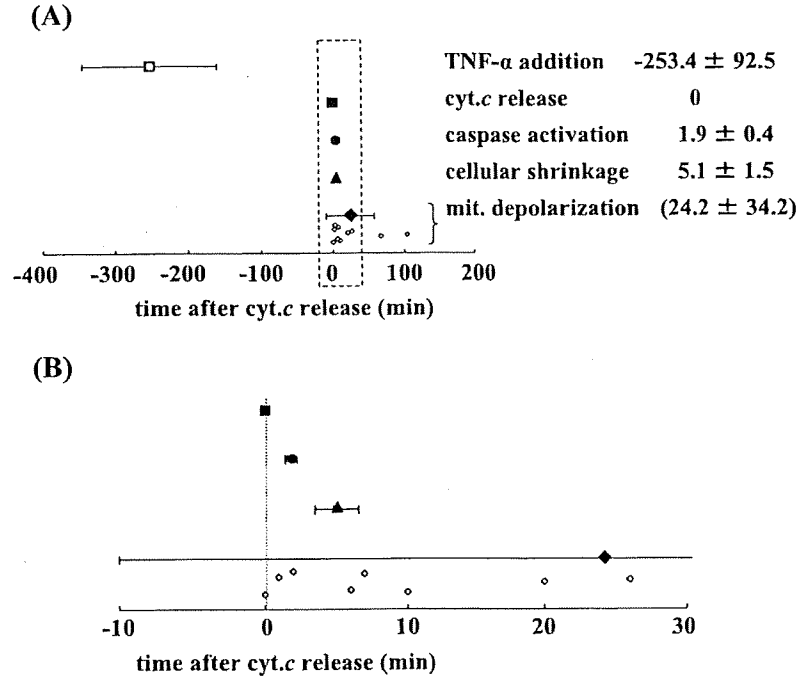

Fig. 3. Temporal relationship between mitochondrial changes and caspase activation. A: Relative timing of TNF-α addition (open square), cyt.*c* release (closed square), caspase activation (closed circle), cellular shrinkage (closed triangle), and mitochondrial depolarization (closed and open diamond) is shown with respect to time after cyt.*c* release. B: Shows a magnification of panel A.

determined as follows: the time point of cyt.*c* release was considered as time 0 in each of the individual cells. We calculated the relative timing of each of the observed events for each cell, and the results are plotted in Fig. 3. TNF-α treatment, cyt.*c* release, caspase activation, and cellular shrinkage are indicated as the mean ± S.D. Since mitochondrial depolarization did not give a normal distribution, all data for mitochondrial depolarization were plotted. Each plot represents the results from a single cell. Figure 3B shows magnification at around time 0.

The relative timing of TNF-α treatment and mitochondrial depolarization was found to deviate substantially, whereas the relative timing of caspase activation and cellular shrinkage gave only a small deviation. A substantial amount of time was required for the initiation of cyt.*c* release, and the duration varied between cells; however, after cyt.*c* release, the subsequent reactions occurred rapidly. After cyt.*c* release, cells are unable to stop or delay the cell death process.

Mitochondrial depolarization occurred before both caspase activation and cellular shrinkage in some of the cells (n = 4), but mitochondrial depolarization occurred after caspase activation and cellular shrinkage in other cells (n = 6). This finding suggests that mitochondrial depolarization is not necessary for either caspase activation or cellular shrinkage. Mitochondrial depolarization has been consistently reported as being associated with cell death, but it is not thought to be a critical step in the induction of apoptotic cell death.

Effects of the duration of TNF-α treatment

At the first step of TNF-α-induced cell death, TNF-α binds with its receptor on the cell surface, and an extracellular signal is transferred into the cell. After this step, Bid transfers the signal to the mitochondria, and then cyt.*c* is released from the mitochondria to the cytosol. Our results shown in Fig. 3 indicate that these processes took about 4 h. In order to analyze the timing of the onset of the earliest steps, we attempted to determine the point in time at which the first step started. To this end, we changed the duration of TNF-α exposure and measured the resulting cell survival rate. Cells were divided to two groups, as shown in Fig. 4A, and the cells were exposed to TNF-α for 0 – 12 h. In group A, the survival rate was measured immediately after TNF-α exposure. In group B, TNF-α was washed off after the indicated exposure time, and the cells were cultured in fresh medium without TNF-α for an additional 6 – 11 h, and the survival rate was then measured. If the cell death process proceeded after the removal of TNF-α, the survival rate would be expected to be reduced due to the additional culture period after the removal of TNF-α. In other words, more cells would be expected to have died in group B than in group A with the same amount of TNF-α exposure time.

The results showed that the survival rate decreased with increasing TNF-α exposure time (Fig. 4B). However, the survival rate did not decrease after TNF-α removal. This result suggests that the dead cells in group B had died during the period of TNF-α exposure, and that those cells that had survived during TNF-α exposure did not die after the removal of TNF-α. Thus, the cell death process is likely to proceed only when the cells were exposed to TNF-α. The survival rate in group B increased when cells were exposed TNF-α for 6 h. The biological meaning of this increase was unknown; however, this result did not disturb our conclusion.

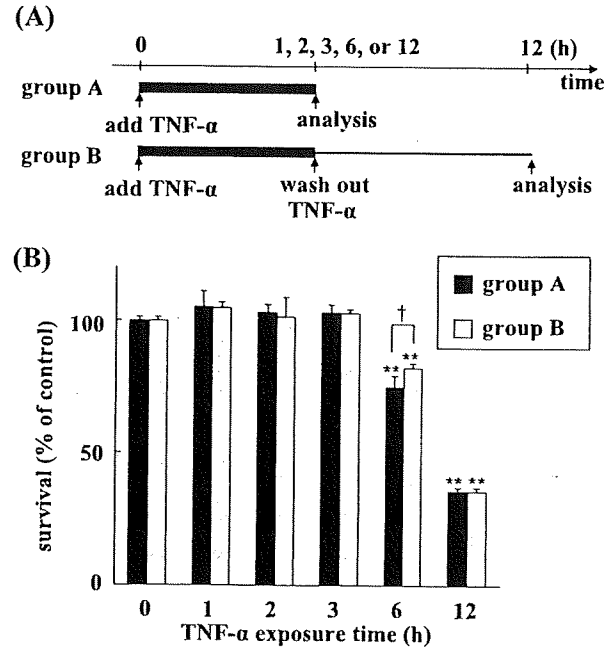

Fig. 4. Cell survival rate after TNF-α exposure. Panel A: Experimental design of the TNF-α exposure analysis. Thick lines represent the incubation in the presence of TNF-α, and thin line represents the incubation in the absence of TNF-α. In group A, cells were exposed to TNF-α for the indicated amount of time, and the cell survival rate was measured immediately. In group B, cells were exposed in the same manner as that used for group A. Then, the TNF-α was washed out, and the cells were cultured in fresh media for 6 – 11 h. Then, the cell survival rate was measured. The total duration of the culture period after the onset of TNF-α exposure was 12 h in group B. Panel B: The cells in groups A and B were exposed to TNF-α for 1, 2, 3, 6, or 12 h, and the cell survival rates were determined. Each bar represents a mean ± S.D. (n = 6). $^{**}P<0.01$ *vs* time 0, according to Dunnett's test. $^{\dagger}P<0.05$ between groups A and B, according to Student's *t*-test.

Discussion

This is the first report to reveal the precise temporal relationships between four reactions (mitochondrial depolarization, cyt.*c* release, caspase activation, and cellular shrinkage) in TNF-α-induced cell death. Because the onset of these reactions varied among individual cells, real-time single-cell imaging is the only currently available method to reveal temporal relationships between these reactions. We described our three-color real-time imaging technique in this report. Rehm et al. has reported the simultaneous real-time imaging of caspase activation and Smac release by using CFP/YFP-FRET sensor and YFP-tagged protein (26). They used the same color, YFP, for the observation of both reactions. It is possible to identify two reactions as they discussed, but it may be difficult to identify small changes occurring in the cell by their method. Previously, we revealed that DsRed was useful for FRET analysis of caspase activation (24). In this report, we observed caspase activation and cyt.*c* release with YFP/DsRed-FRET sensor and CFP-tagged protein. By using fluorescent probes in different colors, each reaction could be easily and precisely identified in a single cell.

We observed cell death at the single-cell level with a resolution period of 0.5 – 1 min, and we revealed that the relative timing between cyt.*c* release, caspase activation, and cellular shrinkage remained constant in all of the dying cells observed; however, the timing of mitochondrial depolarization showed a large deviation (Fig. 3). After cyt.*c* release, apoptosome formation, caspase-9 activation, caspase-3 activation, and the cleavage of various substrates that lead to apoptotic cell death are initiated. Our results revealed that this series of reactions takes place within 10 min and that the time course of this process was identical among all of the dying HeLa cells.

Mitochondrial depolarization was observed in all dying cells, but we considered that mitochondrial depolarization was not the cause of cyt.*c* release, caspase activation, and cellular shrinkage. Mitochondrial depolarization was found to occur at any time after cyt.*c* release. Mitochondrial depolarization was observed after caspase activation and cellular shrinkage in 60% of the observed cells. These results exclude the possibility that mitochondrial depolarization is a cause of cyt.*c* release, caspase activation, and/or cellular shrinkage. This is consistent with previous findings that cell death occurred without mitochondrial depolarization. Li et al. have shown that caspases are activated independently of mitochondrial depolarization in TNF-α-induced cell death (27). Krohn et al. have shown that cyt.*c* release and caspase activation occurred in the absence of mitochondrial depolarization in cell death of hippocampal neurons (28). Several studies suggested that mitochondrial depolarization is a critical step for cell death (29), but our results support the idea that mitochondrial depolarization is not crucial to the cell death process.

Cyt.*c* release may be a key step in two independent series of events, that is, the cell death process and mitochondrial depolarization. We speculate that cells might try to maintain cellular homeostasis by keeping membrane potential after cyt.*c* release. While maintaining the membrane potential, the released cyt.*c* immediately initiated the cell death process in the cytosol, and thus caspase activation and cellular shrinkage always took place within a short period of time. The timing of mitochondrial depolarization did not appear to be relevant to this process.

A number of imaging analyses have demonstrated that each cell death event is a rapid process. Initiator- and effector-caspase activation both proceed rapidly (23, 24, 30 – 32). Cyt.*c* is also released rapidly in a single step (33 – 35). Likewise, Smac/DIABLO is released rapidly, although the duration of Smac/DIABLO release is greater than that of cyt.*c* (26). Several multi-event imaging studies have suggested that cell death events occur almost simultaneously. Initiator caspase activation/effector caspase activation, effector caspase activation/mitochondrial depolarization, cyt.*c*/smac, and effector caspase activation/smac release had been analyzed simultaneously at the single-cell level and were found to occur almost simultaneously (24, 26). These findings, taken together with our present results, suggest that the cell death cascade proceeds rapidly after mitochondrial changes take place.

Once cyt.*c* was released, the following reactions proceed in a rapid manner. However, it did take 253.4 ± 92.5 min from TNF-α treatment to cyt.*c* release, and this duration varied from cell to cell (Figs. 3 and 4). We observed some cells that had died within 1 h in imaging analysis, indicating that cells have the ability to induce cell death within 1 h, and suggesting that certain factors may delay signal transduction and the timing of cell death. The results shown in Fig. 4 indicate that these factors were active only when the cells were exposed to TNF-α. We considered two possible explanations for these findings. 1: Each TNF-α molecule changed the cell slightly, and the changes induced by one molecule were not sufficient to induce the cell death cascade on their own. However, many TNF-α molecules attacked the cell, and intracellular changes thus accumulated. When the accumulated changes exceeded the threshold level, the cell death cascade would be expected to have

proceeded rapidly. 2: TNF-α could induce intracellular changes by chance. According to this explanation, TNF-α molecules would bind with the TNF receptor, but only some of them would be able to induce intracellular change. If some TNF-α molecules successfully induce intracellular changes, then the cell death cascade would proceed rapidly. The more TNF-α molecules that are present around the cell, and/or the longer these TNF-α molecules attack the cell, the higher the probability of a successful attack, and it can be expected that more cells will die. According to both of these models, the cell death process would not proceed in the absence of TNF-α exposure; therefore, those cells that survived during TNF-α exposure would not be expected to die after the removal of TNF-α.

One of the Bcl-2 family proteins, Bid, was cleaved to tBid due to the cell death signal, and the tBid transferred the signal from the cytosol to the mitochondria (36). Exogenous treatment with tBid is known to induce cell death immediately (37), and thus reactions that delay signal transduction may occur at an earlier step than either Bid cleavage or mitochondrial changes.

As cell death reactions often occur in a rapid manner and because the timing of the onset of intracellular reactions varies among cells, precise temporal relationships between cellular events during cell death should be further analyzed at the single-cell level with high temporal resolution. Single-cell imaging analyses of early stages (e.g., receptor oligomerization and the recruitment of adaptor proteins) will help to elucidate the mechanism of the entire cell death process.

Acknowledgments

This study was supported in part by a Grant-in-Aid for Research on Health Sciences focusing on Drug Innovation from the Japan Health Science Foundation; a Grant-in-Aid for Research on Advanced Medical Technology from the Ministry of Health, Labour, and Welfare; and a grant (MF-16) from the Organization for Pharmaceutical Safety and Research.

References

1 Thornberry NA, Lazebnik Y. Caspases: enemies within. Science. 1998;281:1312–1316.
2 Stennicke HR, Salvesen GS. Properties of caspases. Biochim Biophys Acta. 1998;1387:17–31.
3 Boldin MP, Goncharov TM, Goltsev YV, Wallach D. Involvement of MACH, a novel MORT1/FADD-interacting protease, in Fas/APO-1- and TNF receptor-induced cell death. Cell. 1996; 85:803–815.
4 Muzio M, Chinnaiyan AM, Kischkell FC, O'Rourke K, Shevchenko A, Ni J, et al. FLICE, a novel FADD-homologous ICE/CED-3-like protease, is recruited to the CD95 (Fas/APO-1) death-inducing signal complex. Cell. 1996;85:817–827.
5 Medema JP, Scaffidi C, Kischkel FC, Shevchenko A, Mann M, Krammer PH, et al. FLICE is activated by association with the CD95 death-inducing signaling complex (DISC). EMBO J. 1997;16:2794–2804.
6 Martin DA, Siegel RM, Zheng L, Lenardo MJ. Membrane oligomerization and cleavage activates the caspase-8 (FLICE /MACHalpha1) death signal. J Biol Chem. 1998;273:4345–4349.
7 Srinivasula SM, Ahmad M, Fernandes-Alnemri T, Litwack G, Alnemri ES. Molecular ordering of the Fas-apoptotic pathway: The Fas/APO-1 protease Mch5 is a CrmA-inhibitable protease that activates multiple Ced-3/ICE-like cysteine proteases. Proc Natl Acad Sci U S A. 1996;93:14486–14491.
8 Orth K, O'Rourke K, Salvesen GS, Dixit VM. Molecular ordering of apoptotic mammalian CED-3/ICE-like proteases. J Biol Chem. 1996;271:20977–20980.
9 Tewari M, Quan LT, O'Rourke K, Desnoyers S, Zeng Z, Beidler DR, et al. Yama/CPP32 beta, a mammalian homolog of CED-3, is a CrmA-inhibitable protease that cleaves the death substrate poly(ADP-ribose) polymerase. Cell. 1995;81:801–809.
10 Green DR, Reed JC. Mitochondria and apoptosis. Science. 1998;281:1309–1312.
11 Martinou JC, Green DR. Breaking the mitochondrial barrier. Nat Rev Mol Cell Biol. 2001;2:63–67.
12 Saleh A, Srinivasula SM, Acharya S, Fishel R, Alnemri ES. Cytochrome c and dATP-mediated oligomerization of Apaf-1 is a prerequisite for procaspase-9 activation. J Biol Chem. 1999;274:17941–17945.
13 Shiozaki EN, Chai J, Shi Y. Oligomerization and activation of caspase-9, induced by Apaf-1 CARD. Proc Natl Acad Sci U S A. 2002;99:4197–4202.
14 Tyas L, Brophy VA, Pope A, Rivett AJ, Tavare JM. Rapid caspase-3 activation during apoptosis revealed using fluorescence-resonance energy transfer. EMBO reports. 2000;1:266–270.
15 Rehm M, Dussmann H, Janicke RU, Tavare JM, Kogel D, Prehn JHM. Single-cell fluorescence resonance energy transfer analysis demonstrates that caspase activation during apoptosis is a rapid process: role of caspase-3. J Biol Chem. 2002;277: 24506–24514.
16 Luo KQ, Yu VC, Pu Y, Chang DC. Application of the fluorescence resonance energy transfer method for studying the dynamics of caspase-3 activation during UV-induced apoptosis in living HeLa cells. Biochem Biophys Res Commun. 2001;283:1054–1060.
17 Morgan MJ, Thorburn A. Measurement of caspase activity in individual cells reveals differences in the kinetics of caspase activation between cells. Cell Death Differ. 2001;8:38–43.
18 Tsien RY, Miyawaki A. Seeing the machinery of live cells. Science. 1998;280:1954–1955.
19 Miyawaki A, Sawano A, Kogure T. Lighting up cells: labeling proteins with fluorophores. Nat Cell Biol. 2003;S1–S7.
20 Tsien RY, The green fluorescent protein. Annu Rev Biochem. 1998;67:509–544.
21 Erickson MG, Moon DL, Yue DT. DsRed as a potential FRET partner with CFP and GFP. Biophys J. 2003;85:599–611.
22 Karasawa S, Araki T, Nagai T, Mizuno H, Miyawaki A. Cyan-emitting and orange-emitting fluorescent proteins as a donor

/acceptor pair for fluorescence resonance energy transfer. Biochem J. 2004;381:307–312.

23 Kawai H, Suzuki T, Kobayashi T, Mizuguchi H, Hayakawa T, Kawanishi T. Simultaneous imaging of initiator/effector caspase activity and mitochondrial membrane potential during cell death in living HeLa cells. Biochim Biophys Acta. 2004;1693:101–110.

24 Kawai H, Suzuki T, Kobayashi T, Sakurai H, Ohata H, Honda K, et al. Simultaneous real-time detection of initiator- and effector-caspase activation by double fluorescence resonance energy transfer analysis. J Pharmacol Sci. 2005;97:361–368.

25 Scaduto RC Jr, Grotyohann LW. Measurement of mitochondrial membrane potential using fluorescent rhodamine derivatives. Biophys J. 1999;76:469–477.

26 Rehm M, Dussmann H, Prehn JHM. Real-time single cell analysis of Smac/DIABLO release during apoptosis. J Cell Biol. 2003;162:1031–1043.

27 Li X, Du L, Darzynkiewicz Z. During apoptosis of HL-60 and U-937 cells caspases are activated independently of dissipation of mitochondrial electrochemical potential. Exp Cell Res. 2000;257:290–297.

28 Krohn AJ, Wahlbrink T, Prehn JHM. Mitochondrial depolarization is not required for neuronal apoptosis. J Neurosci. 1999;19:7394–7404.

29 Heiskanen KM, Bhat MB, Wang H-W, Ma J, Nieminen A-L. Mitochondrial depolarization accompanies cytochrome c release during apoptosis in PC6 cells. J Biol Chem. 1999;274:5654–5658.

30 Ohnuki R, Nagasaki A, Kawasaki H, Baba T, Uyeda TQP, Taira K. Confirmation by FRET in individual living cells of the absence of significant amyloid β-mediated caspase 8 activation. Proc Natl Acad Sci U S A. 2002;99:14716–14721.

31 Takemoto K, Nagai T, Miyawaki A, Miura M. Spatio-temporal activation of caspase revealed by indicator that is insensitive to environmental effects. J Cell Biol. 2003;160:235–243.

32 Luo KQ, Yu VC, Pu Y, Chang DC. Measuring dynamics of caspase-8 activation in a single living HeLa cell during TNFalpha-induced apoptosis. Biochem Biophys Res Commun. 2003;304:217–222.

33 Lim MLR, Lum M-G, Hansen TM, Roucou X, Nagley P. On the release of cytochrome c from mitochondria during cell death signaling. J Biomed Sci. 2002;9:488–506.

34 Goldstein JC, Waterhouse NJ, Juin P, Evan GI, Green DR. The coordinate release of cytochrome c during apoptosis is rapid, complete and kinetically invariant. Nat Cell Biol. 2000;2:156–162.

35 Goldstein JC, Munoz-Pinedo C, Ricci J-E, Adams SR, Kelekar A, Schuler M, et al. Cytochrome c is released in a single step during apoptosis. Cell Death Differ. 2005;12:453–462.

36 Luo X, Budihardjo I, Zou H, Slaughter C, Wang X. Bid, a Bcl-2 interacting protein, mediates cytochrome c release from mitochondria in response to activation of cell surface death receptors. Cell. 1998;94:481–490.

37 Madesh M, Antonsson B, Srinivasula SM, Alnemri ES, Hajnóczky G. Rapid kinetics of tbid-induced cytochrome c and Smac/DIABLO release and mitochondrial depolarization. J Biol Chem. 2002;277:5651–5659.

Available online at www.sciencedirect.com
ScienceDirect
Biologicals xx (2007) 1–11
BIOLOGICALS
www.elsevier.com/locate/biologicals

Influences of the recombinant artificial cell adhesive proteins on the behavior of human umbilical vein endothelial cells in serum-free culture

Akiko Ishii-Watabe [a,*], Toshie Kanayasu-Toyoda [b], Takuo Suzuki [a], Tetsu Kobayashi [a], Teruhide Yamaguchi [b], Toru Kawanishi [a]

[a] Division of Biological Chemistry and Biologicals, National Institute of Health Sciences, 1-18-1 Kamiyoga, Setagaya-ku, Tokyo 158-8501, Japan
[b] Division of Cellular and Gene Therapy Products, National Institute of Health Sciences, 1-18-1 Kamiyoga, Setagaya-ku, Tokyo 158-8501, Japan

Received 8 June 2006; revised 4 December 2006; accepted 22 December 2006

Abstract

To improve the safety of cellular therapy products, it is necessary to establish a serum-free cell culture method that can exclude animal-derived materials in order to avoid contamination with transmissible agents. It would be optimal if the proteins necessary to a serum-free culture could be provided as recombinant proteins. In this study, the influences of recombinant artificial cell adhesive proteins on the behavior of human umbilical vein endothelial cells (HUVECs) in serum-free culture were examined in comparison with the influence of plasma fibronectin (FN). The recombinant proteins used were Pronectin F (PF), Pronectin F PLUS (PFP), Pronectin L (PL), Retronectin (RN), and Attachin (AN). HUVECs adhered more efficiently on PF or PFP than on FN. No cells adhered on PL. Regarding the VEGF or bFGF-induced cell growth, the cells on PF and PFP proliferated at a similar rate to the cells on FN. RN and AN were less effective in supporting cell growth. Since cell adhesion on PF and PFP induced phosphorylation of focal adhesion kinase, they are thought to activate integrin-mediated intracellular signaling. The cells cultured on PF or PFP were able to produce prostaglandin I_2 or tissue-plasminogen activator in response to thrombin. However, thrombin caused detachment of the cells from PF but not from PFP or FN, meaning that the cells were able to adhere more tightly on PFP or FN than on PF. These data indicate that PFP could be applicable as a substitute for plasma FN.

Keywords: Cell adhesive protein; Recombinant protein; Fibronectin; Endothelial cells

1. Introduction

The widespread development of cellular therapy products has advanced to the stage of non-clinical and clinical testing [1–3]. Regulatory documents for human somatic cell therapy including instructions for investigational new drug applications have been published [4–6]. To guarantee the safety of both product recipients and the public at large, it is crucial to prevent contamination of cellular therapy products by infectious agents [7].

Serum-free culture is one of the desired methods for manufacturing cellular therapy products when safety issues are a concern [8,9]. Although serum is a very effective additive for a culture medium that can support cell adhesion, survival, growth, and functions, animal-derived materials such as serum may contain transmissible agents or human allergens [10–13]. Since serum is composed of proteins, sugars, lipids, vitamins, and other ingredients, its quality is affected by the genetic and environmental circumstances of the animal used, which means there are lot-to-lot variations in composition and potency. This variability could reduce the consistency of cellular therapy products, and a serum-free culture that could contribute to improving the consistency of the cell features is thus needed.

Protein factors often need to be added to serum-free culture to substitute for the functions of serum. The proteins used for this purpose must also pose no risk of infection. Because recombinant proteins can be produced without using animal-derived materials, and pose little risk of contaminating human pathogens, they are a useful biomaterial for culturing cells

* Corresponding author. Tel./fax: +81 3 3700 9084.
E-mail address: watabe@nihs.go.jp (A. Ishii-Watabe).

1045-1056/07/$32.00 © 2007 The International Association for Biologicals. Published by Elsevier Ltd. All rights reserved.
doi:10.1016/j.biologicals.2006.12.002

when safety issues are a concern. In addition, the functions of recombinant proteins can be improved by modifying their amino acid sequences, which is also an advantage. In this study, using a serum-free culture of human umbilical vein endothelial cells (HUVECs), the usefulness of recombinant artificial cell adhesive proteins as a plasma fibronectin substitute was evaluated.

The extracellular matrix glycoprotein fibronectin consists of two similar polypeptide chains, each with a molecular mass of approximately 250 kDa joined at their respective C termini by disulfide bonds [14,15]. The RGD (arginine–glycine–aspartic acid) recognition sequence located within the molecule was the first amino acid motif shown to mediate cell adhesion [16,17]. Intracellular signaling induced by cell adhesion on fibronectin plays a critical role in cytoskeletal reorganization, cell cycle progression, and cell survival [18,19].

This study defines the influences of five different kinds of recombinant artificial cell adhesive proteins on endothelial adhesion, proliferation, and antithrombotic function in serum-free culture for which plasma fibronectin is needed. The recombinant proteins used were Pronectin F, Pronectin F PLUS, Pronectin L, Retronectin, and Attachin (Table 1).

2. Materials and methods

2.1. Recombinant cell adhesive proteins

Pronectin F, Pronectin F PLUS, and Pronectin L were purchased from Sanyo Chemical Industry (Kyoto, Japan), Retronectin from TaKaRa (Shiga, Japan), and Attachin from Bio999 (Taipei, Taiwan). All of these proteins were produced via bacterial fermentation. Pronectin F is a genetically engineered protein containing repeating units of the RGD sequence interspersed with a β-silk peptide for structural stability [20]. It is comprised of 980 amino acids. Based on its sequence, the molecular weight is estimated to be 72,728. The amino acid sequence is fMDPVVLQRRDWENPGVTQLNRLAA HPPFASDPMGAGS(GAGAGS)$_6$GAAVTGRGDSPASAAGY-[(GAGAGS)$_9$GAAVTGRGDSPASAAGY]$_{12}$-(GAGAGS)$_2$GA GAMDPGRYQLSAGRYHYQLVWCQK. Pronectin F PLUS is a positively charged water-soluble variant of Pronectin F that is produced by chemical modification [21,22]. Pronectin L is a protein polymer that exhibits IKVAV epitopes from the laminin alpha chain with a similar backbone as Pronectin F [21]. It is comprised of 1019 amino acids. The molecular weight is estimated to be 75,639. The amino acid sequence is fMDPVVLQRRDWENPGVTQLNRLAAHPPFASDPMGA GS(GAGAGS)$_6$GAAPGASIKVAVSAGPSAGY-[(GAGAGS)$_9$ GAAPGAIKVAVSAGPSAGY]$_{12}$-(GAGAGS)$_2$GAGAMDPG RYQLSAGRYHYQLVWCQK. Retronectin consists of a central cell-binding domain, a high affinity heparin-binding domain II, and a CS1 site within an alternatively spliced type III connecting segment region of human fibronectin [23]. It is comprised of 574 amino acids. The molecular weight is estimated to be 62,631. Attachin is an artificial fusion protein with the molecular weight of 30 kDa that has several functional domains, including a fibronectin-like cell attachment domain [24]. It has reportedly been used to promote the adhesion of several kinds of cell lines, including CHO-K1, MDBK, PK-15, L929, Vero, COS, U373, Swiss 3T3, and MRC-5 [25].

2.2. Cells and materials

Human umbilical vein endothelial cells (HUVECs) were purchased from Sanko Junyaku (Tokyo, Japan) and maintained

Table 1
Fibronectin and recombinant cell adhesive proteins used in this study

Proteins	Structure	Molecular Weight
Fibronectin	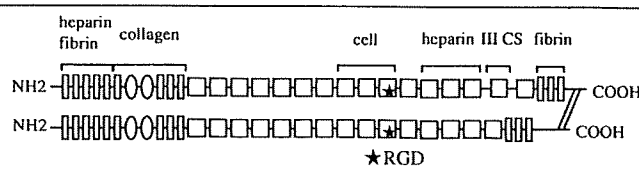	250K x 2
Pronectin F	Head-[(GAGAGS)$_9$GAAVTGRGDSPASAAGY]$_{12}$-Tail ★	73K
Pronectin F Plus	Positively charged, water-soluble variant of Pronectin F	73K
Pronectin L	Head-[(GAGAGS)$_9$GAAPGASIKVAVSAGPSAGY]$_{12}$-Tail ◆	76K
Retronectin	Chimeric protein of human fibronectin fragment 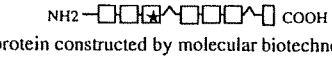	63K
Attachin	A fusion protein constructed by molecular biotechnology	30K

Fibronectin.
▯ Type I module.
() Type II module.
□ Type III module.
★: cell attachment sequence derived from fibronectin.
◆: cell attachment sequence derived from laminin.

Please cite this article in press as: Ishii-Watabe A et al., Influences of the recombinant artificial cell adhesive proteins on the behavior of human umbilical vein endothelial cells in serum-free culture, Biologicals (2007), doi:10.1016/j.biologicals.2006.12.002

in EGM-2 media (Cambrex, Walkersville, MD) on collagen-coated dishes (Asahi Techno Glass, Tokyo, Japan). EGM-2 media is modified MCDB 131 containing 2% fetal bovine serum, VEGF, bFGF, IGF-1, EGF, heparin, hydrocortisone and ascorbic acid. The cells were kept in a humidified, 5% CO_2 environment at 37 °C. Cells between passages 3 and 5 were used for all experiments.

The serum-free media used was human endothelial SFM (Invitrogen, Carlsbad, CA) [26]. Ten nanograms/ml of epidermal growth factor (EGF) (Invitrogen) and 20 ng/ml of basic fibroblast growth factor (bFGF) (Invitrogen) were added as supplements. Fibronectin is recommended for use as a cell attachment factor.

2.3. Cell adhesion assay

Recombinant cell adhesive proteins were diluted with phosphate buffered saline (PBS(−)), and plated on multiwell non-treated polystyrene plates (BD Falcon, Franklin Lakes, NJ). The plates were incubated for 2 h at room temperature, and then the protein solutions were removed and the wells washed with PBS(−). The concentration of the recombinant proteins used was 10 μg/ml (2 μg/cm^2), unless the description states otherwise. The amount of absorbed protein was quantified with a QuantiPro BCA Kit (Sigma, St. Louis, MO) using bovine serum albumin as a standard.

The HUVECs were harvested using trypsin and washed twice with PBS(−). The cells were then suspended in serum-free media, and added to each well of 96-well plates previously coated with recombinant cell adhesion proteins at a cell density of 1×10^4 cells/well. After incubating for 60 min under 5% CO_2 at 37 °C, the supernatant was removed, and the wells rinsed with PBS(−) to remove non-adherent cells. Following fixation of the adherent cells by 4% paraformaldehyde for 10 min, the paraformaldehyde was removed and the cells washed once with distilled water. A 0.5% (w/v) solution of crystal violet was then added to the wells. After staining for 25 min, the cells were rinsed five times with distilled water and the crystal violet that was absorbed on the adherent cells was solubilized with 0.5% SDS. The optical density at 595 nm was measured on an EL340 plate reader (BioTek Instruments, Winooski, VT).

2.4. Measurement of cell proliferation

HUVECs were harvested and suspended in serum free media, and plated to each well of the 96-well plates previously coated with recombinant cell adhesive proteins. VEGF (R&D Systems, Minneapolis, MN) or bFGF (Invitrogen, Carlsbad, CA) was added at concentrations of 1−100 ng/ml. After culturing for 2 days under 5% CO_2 at 37 °C, the cell number in each well was measured using Cell Counting Kit-8 (Dojindo, Kumamoto, Japan). Results are expressed as the mean value ± S.D. of triplicate determinations.

2.5. Phosphorylation of focal adhesion kinase

The HUVECs were collected by trypsin treatment (Invitrogen), resuspended in serum free medium, incubated for 2 h at 37 °C in suspension, and subsequently plated at 5×10^5 cells/dish on 60 mm diameter dishes pre-coated with cell adhesive proteins or bovine serum albumin (BSA) (10 μg/ml) [27]. After incubation for 2 h under 5% CO_2 at 37 °C, the cells were lysed in RIPA buffer (50 mM Tris–HCl (pH 7.6), 150 mM NaCl, 1% NP-40, 0.25% sodium deoxycholate), and the protein concentrations were determined using the BCA assay (Pierce, Rockford, IL). 3.5 μg of the total cell lysates was resolved by SDS–PAGE, blotted onto Immobilon-P membranes (Millipore, Volketswil, Switzerland), and incubated in 1% BSA with anti-pY397 FAK antibody (Upstate Biotechnology Inc.,, Lake Placid, NY) followed by incubation with horseradish peroxidase-labeled secondary antibody (Cell Signaling Technology, Danvers, MA). The ECL system (GE Healthcare Bio-Sciences AB, Uppsala, Sweden) and Luminoimage analyzer LAS 3000 (Fuji Film, Kanagawa, Japan) were used for detection. The membranes were stripped of bound antibody using a Re-Blot Plus Western Blot Recycling Kit (Chemicon, Temecula, CA), and the membrane was reprobed with anti-FAK antibody (Upstate Biotechnology). The labeled bands were quantified using the MultiGauge software program (Science Lab). The quantified value for phosphorylated FAK was normalized with that for total FAK in each sample, and the relative phosphorylation level was then calculated as a ratio against the cell lysate on fibronectin.

2.6. Secretion of Prostaglandin I_2 (PGI_2)

The HUVECs were harvested using trypsin, washed twice, and then suspended in serum-free media. The cells were placed on the 24-well plates coated with recombinant cell adhesive proteins at the density of 7×10^4/well. After culturing for 1 day, the cells were stimulated with 1 U/ml of thrombin or 30 ng/ml of VEGF. The cells were incubated for 1 h under 5% CO_2 at 37 °C, and then the supernatant was collected. The supernatant was centrifuged for 10 min at 2000 × g in a microcentrifuge to remove any residual cells. The level of 6-keto Prostaglandin $F_1\alpha$, a major metabolite of Prostaglandin I_2, was determined using 6-keto Prostaglandin $F_1\alpha$ EIA Kit (Cayman Chemical, Ann Arbor, MI). Each culture condition was repeated in triplicate.

2.7. Secretion of tissue-plasminogen activator

The HUVECs were seeded as described above. After culturing for 1 day, the cells were stimulated with 0.01−1 U/ml of thrombin. Twenty-four hours later, the supernatant was collected and spun down for 10 min at 2000 × g in a microcentrifuge. The level of tissue plasminogen activator was determined using the AssayMax Human Tissue-Type Plasminogen Activator ELISA Kit (Assay Pro, Brooklyn, NY). Each culture condition was repeated in triplicate. Phase contrast images were obtained before the supernatant was collected.

Please cite this article in press as: Ishii-Watabe A et al., Influences of the recombinant artificial cell adhesive proteins on the behavior of human umbilical vein endothelial cells in serum-free culture, Biologicals (2007), doi:10.1016/j.biologicals.2006.12.002

3. Results

3.1. Adhesion of HUVECs onto recombinant cell adhesive proteins

To examine the adhesion onto the recombinant cell adhesive proteins, HUVECs harvested and suspended in serum-free media were applied on plastic wells precoated with Pronectin F, Pronectin F PLUS, Pronectin L, Retronectin, Attachin, or fibronectin (Table 1). As shown in Fig. 1, Pronectin F, Pronectin F PLUS, Retronectin, or Attachin showed cell adhesion activity to a similar extent as fibronectin at the concentration of 10 μg/ml (2 μg/cm^2). Pronectin F and Pronectin F PLUS were superior to fibronectin when they were used at an amount of less than 1 μg/ml. The cells were observed under microscopy to have spread well on the recombinant proteins that they adhered to (Fig. 2). No cells had adhered onto Pronectin L or BSA.

In order to test if these differences are due to the difference in the absorbed amount of each protein, the protein absorbed on the plate was measured (Fig. 3). It was found that Pronectin F and Pronectin L had absorbed to the plate better than other proteins and that the absorbed amount of Pronectin F PLUS was lower than that of Pronectin F and Pronectin L. From the point of view of the efficiency of cell adhesion (Fig. 1) and the absorbed amount of protein (Fig. 3), the number of cells attached was not dependent on the amount of absorbed protein, suggesting that the observed effects were not due to differences in protein absorption but rather due to the character of each cell adhesion protein.

3.2. Influences on cell proliferation

Besides anchorage, cell adhesion to components of the extracellular matrix triggers signaling events affecting diverse cellular traits and activities, including survival, proliferation, and other functions. Therefore, the influences of the recombinant cell adhesion proteins on cell proliferation were examined. The HUVECs in serum-free media were seeded on the plates that were coated with recombinant cell adhesive proteins, and then cultured in the presence or absence of basic fibroblast growth factor (bFGF) or vascular endothelial growth factor (VEGF) at concentrations from 1 to 100 ng/ml. After culturing for 2 days, the cell numbers in each well were examined (Fig. 4). When HUVECs were cultured in the presence of bFGF, the cells on Pronectin F or Pronectin F PLUS had grown to the same level as that on fibronectin in each concentration of bFGF, showing that Pronectin F and Pronectin F PLUS have the same growth support potency as fibronectin (Fig. 4A). However, the cell numbers on Retronectin or Attachin reached 70% or 40% of that on fibronectin, respectively; showing that the growth support potency of Retronectin and Attachin was lower than fibronectin. When VEGF-stimulated cell proliferation was examined, Pronectin F and Pronectin F PLUS also showed similar growth-supporting potency to fibronectin (Fig. 4B). Retronectin and Attachin were less effective than fibronectin.

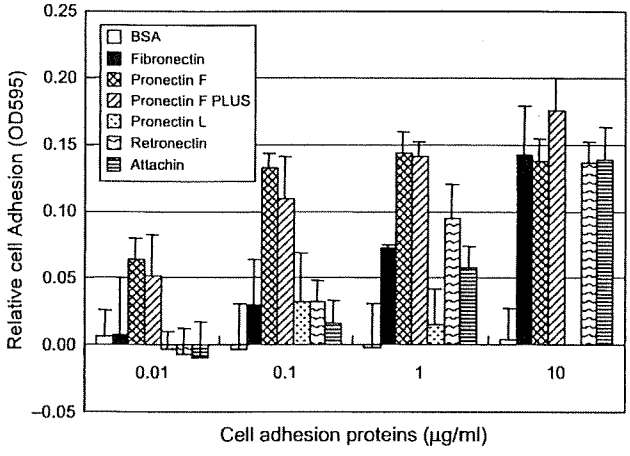

Fig. 1. Adhesion of HUVECs to recombinant cell adhesive proteins. HUVECs were plated into wells previously coated with Fibronectin, Pronectin F, Pronectin F PLUS, Pronectin L, Retronectin, Attachin, or BSA, and then incubated for 1 h at 37 °C. Attached cells were fixed and stained with crystal violet and quantified by absorbance reading. Results are expressed as mean value ± S.D. of triplicate determinations. The 0.1 OD corresponded to 0.61 ± 0.085 × 10^4 cells.

3.3. Phosphorylation of focal adhesion kinase

Cell adhesive proteins activate intracellular signaling via cell surface integrins. In regulating the cellular responses to integrin-mediated adhesion, focal adhesion kinase (FAK) has emerged as a key signaling molecule [28–30]. Integrin–ligand engagement promotes FAK tyrosine phosphorylation that promotes FAK signaling activity. The phosphorylation of FAK Tyr-397, the only apparent autophosphorylation site, is known to create a high-affinity binding site for SH2 domains of the Src-family kinases, including c-Src and Fyn [31].

HUVECs cultured in growing media were harvested by trypsin treatment, and incubated in serum-free media for 2 h at 37 °C in suspension. After this incubation, the cells were plated onto the dishes in which recombinant cell adhesive proteins were coated, and then incubated for 2 h under 5% CO_2 at 37 °C. Cell lysates were prepared using RIPA buffer, and the phosphorylation level of FAK on Tyr 397 was then examined by Western blotting. As shown in Fig. 5, FAK Tyr-397 is phosphorylated under an attached condition (lane 1), becomes dephosphorylated upon cell suspension (lane 2), and then becomes rephosphorylated after replating. The FAK phosphorylation level after replating on recombinant proteins differed in each sample (lanes 3–10). Phosphorylation level of cells on BSA (lane 3) or Pronectin L (lane 7), to which cells did not adhere, was still lower after replating. Pronectin F (lane 5) or Pronectin F PLUS (lane 6) induced FAK phosphorylation to the similar extent to Fibronectin (lane 4), suggesting that Pronectin F and Pronectin F PLUS are thought to activate intracellular signaling via integrin as well as fibronectin. Retronectin that has RGD domain of Fibronectin also induced FAK phosphorylation (lane 8).

Please cite this article in press as: Ishii-Watabe A et al., Influences of the recombinant artificial cell adhesive proteins on the behavior of human umbilical vein endothelial cells in serum-free culture, Biologicals (2007), doi:10.1016/j.biologicals.2006.12.002

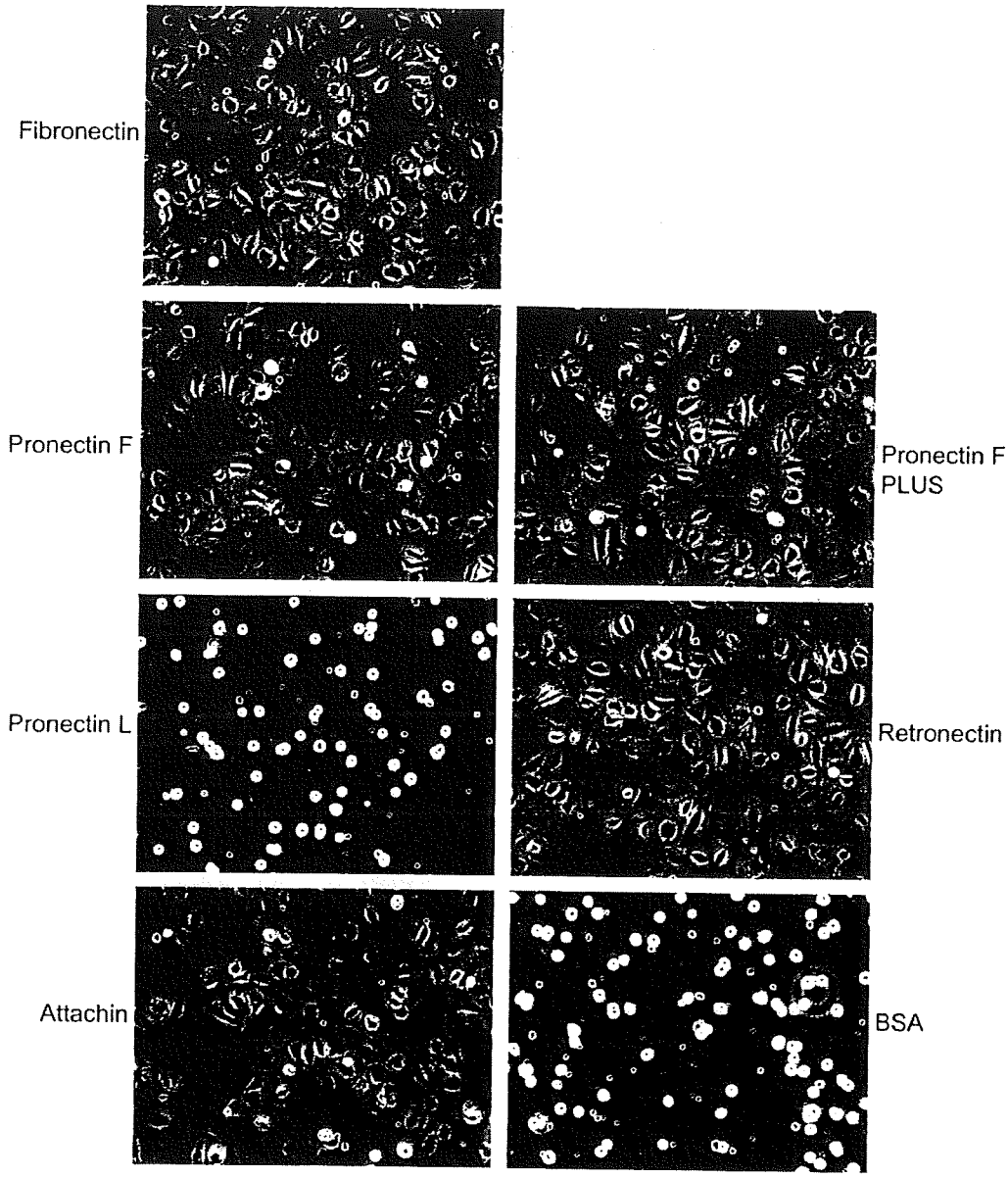

Fig. 2. The phase contrast images of cell attachment and spreading on recombinant cell adhesive proteins. HUVECs were seeded into wells previously coated with 10 μg/ml of Fibronectin, Pronectin F, Pronectin F PLUS, Pronectin L, Retronectin, Attachin, or BSA. After 1 h incubation at 37 °C, the cells were photographed with an inverted microscope.

3.4. Influences on antithrombotic functions of endothelial cells

In order to examine the influences of recombinant cell adhesive proteins on cellular functions, the production of prostaglandin I_2 (PGI_2) and tissue-plasminogen activator (t-PA), both of which play important roles in the antithrombotic feature of endothelial cells, was tested. Antithrombotic activity is the most important characteristic of endothelial cells that are used for artificial blood vessels or engineered vascularized tissues. PGI_2 inhibits platelet aggregation, thereby inhibiting the formation of thrombus. It is produced quickly after stimulation via the activation of phospholipase A_2. Since the half life of PGI_2 is as short as 2 min, the concentrations of its metabolite 6-keto Prostaglandin $F_1\alpha$ were measured. t-PA is produced from endothelial cells via the induction of protein synthesis in response to the extracellular stimuli. It induces the processing of plasminogen to plasmin, and dissolves the fibrin clots.

HUVECs were plated on the recombinant cell adhesion protein-coated dishes and cultured for 1 day, then stimulated with VEGF or thrombin. As shown in Fig. 6A, PGI_2 was produced from VEGF- stimulated HUVECs on different kinds of cell adhesive proteins to the same level. In the serum-free media, the basal production of PGI_2 was higher, and the production after the stimulation was less than in the growing

Please cite this article in press as: Ishii-Watabe A et al., Influences of the recombinant artificial cell adhesive proteins on the behavior of human umbilical vein endothelial cells in serum-free culture, Biologicals (2007), doi:10.1016/j.biologicals.2006.12.002

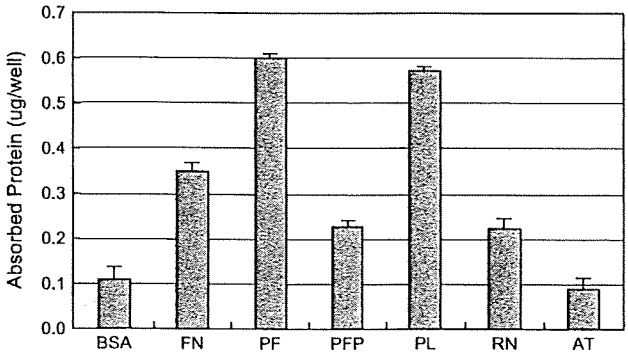

Fig. 3. Protein absorption on non-treated polystyrene plates. Ten μg/ml of bovine serum albumin (BSA), Fibronectin (FN), Pronectin F (PF), Pronectin F PLUS (PFP), Pronectin L (PL), Retronectin (RN) or Attachin (AN) was added to 96-well plates and incubated at room temperature for 2 h. Each well was washed with PBS(−) and the amount of absorbed protein was quantitated by QuantiPro BCA using bovine serum albumin as a standard. Each data point represents the mean ± S.D. of triplicate determinations.

media. Similar results were obtained when the cells were stimulated with thrombin (Fig. 6B).

Next, t-PA production from the thrombin-stimulated HUVECs was examined. As shown in Fig. 7, the t-PA concentration in the culture supernatant of HUVECs that adhered on Pronectin F PLUS was the same as that on Fibronectin. However, the concentration was lower in the supernatant on Pronectin F, Retronectin, or Attachin than on fibronectin. The basal production of t-PA in the serum-free media was less than in growing media; therefore, responsiveness to thrombin was readily observed in the serum-free culture.

During these experiments using thrombin, detachment of the thrombin-stimulated cells from Pronectin F, Retronectin, or Attachin was observed (Fig. 8). No detachment was seen in the cells that adhered on fibronectin or Pronectin F PLUS. This result might reflect the possibility that the adhesiveness of the cells to Pronectin F, Retronectin, and Attachin is weaker than to Pronectin F PLUS or fibronectin.

The following data support the results of Fig. 8, which are presented using microscopic images. Since HUVECs are adherent cells, detachment from the dishes leads to a loss of viability. Therefore, changes in the viable cell concentration after thrombin stimulation reflect cell detachment. As shown in Fig. 9, the production of t-PA and changes in the viable cell concentration after culturing in the presence of 0.01, 0.1, or 1 U/ml of thrombin were tested. At all three concentrations of thrombin used, cell detachment was observed only from Pronectin F. Although the t-PA concentration was increased in a dose-dependent manner by thrombin in the cells that adhered on Fibronectin or Pronectin F PLUS (Fig. 9A), there was less of an increase in t-PA production from the cells on Pronectin F when a low dose (0.01 or 0.1 U/ml) of thrombin was used. At those concentrations, the viable cell concentration on Pronectin F was decreased by thrombin stimulation, meaning that cell detachment occurred on Pronectin F (Fig. 9B). At a high concentration of thrombin (1 U/ml), the viable cell concentration decreased slightly even though cell detachment was

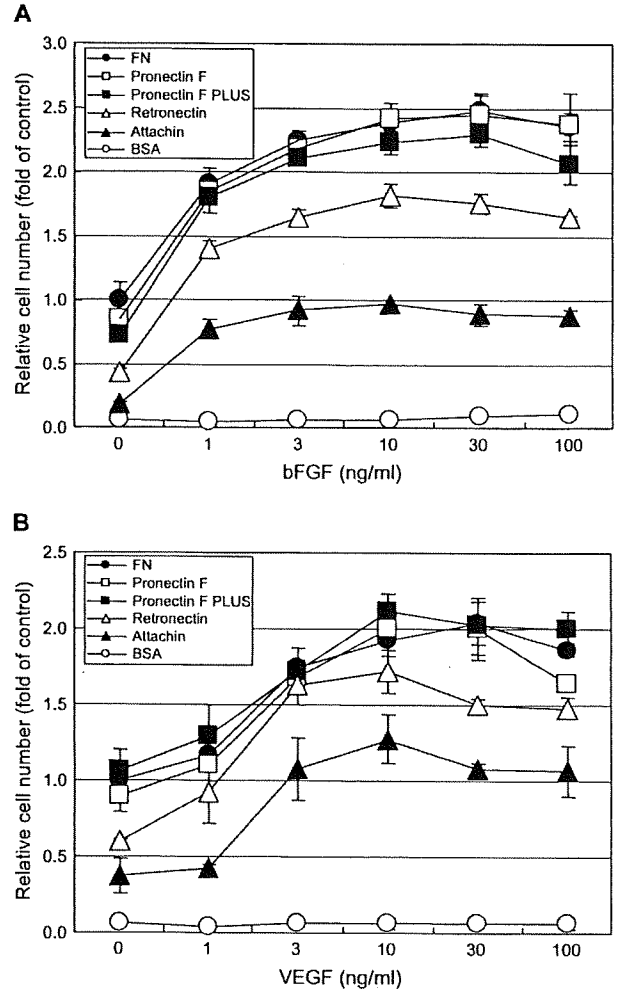

Fig. 4. Effects of recombinant cell adhesive proteins on the VEGF- or bFGF-induced cell proliferation. HUVECs were seeded into wells previously coated with 10 μg/ml of Fibronectin, Pronectin F, Pronectin F PLUS, Retronectin, Attachin, or BSA, and cultured for 2 days in the presence or absence of bFGF (A) or VEGF (B) at the concentrations indicated. The relative cell number was examined using a cell counting kit-8. The results are expressed as the mean value ± S.D. of triplicate determinations.

observed. This might be because the cell proliferative effect of thrombin canceled the decrease in cell viability. t-PA production corrected by the viable cell concentration is shown in Fig. 9C. By correcting the t-PA concentration using the viable cell concentration, the dose-dependency of thrombin in t-PA production was similar in Pronectin F to Pronectin F PLUS and fibronectin (Fig. 9C). From these results, in the cells on Pronectin F and Pronectin F PLUS, the signals from thrombin transduced similarly, but the strength of the cell adhesion differed.

4. Discussion

The goal of the present study was to establish a cell culture method that can improve the safety of cellular therapy products. Our focus is now on human endothelial cells, because

Please cite this article in press as: Ishii-Watabe A et al., Influences of the recombinant artificial cell adhesive proteins on the behavior of human umbilical vein endothelial cells in serum-free culture, Biologicals (2007), doi:10.1016/j.biologicals.2006.12.002

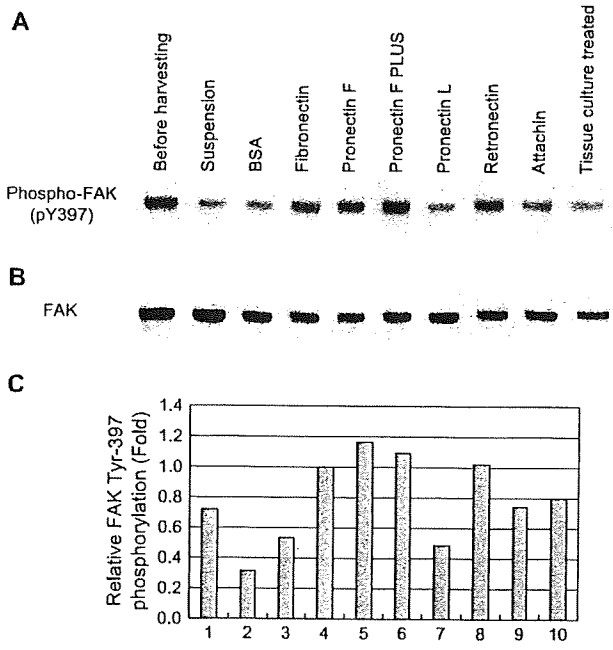

Fig. 5. FAK activation in HUVECs adhered to recombinant cell adhesive proteins. HUVECs cultured in serum-containing EGM-2 media on collagen-coated plates were harvested and held in suspension for 2 h at 37 °C, then plated onto precoated plates with 10 μg/ml of Fibronectin, Pronectin F, Pronectin F PLUS, Pronectin L, Retronectin, or Attachin. After 2 h incubation at 37 °C, cell lysates were prepared using RIPA buffer. The cell extracts were analyzed for the phosphorylation (A) and protein levels of focal adhesion kinase (B) by Western blotting. The amount of proteins detected was analyzed using MultiGauge software (C). Lane 1: before harvesting; lane 2: after suspension; lane 3: BSA; lane 4: Fibronectin; lane 5: Pronectin F; lane 6: Pronectin F PLUS; lane 7: Pronectin L; lane 8: Retronectin; lane 9: Attachin; lane 10: tissue culture-treatment dish. Similar results were obtained in two independent experiments. Representative blots are shown.

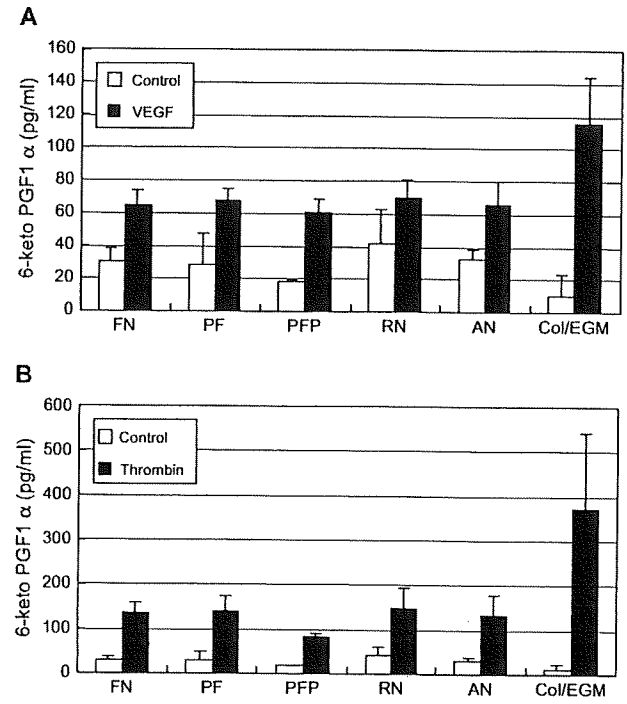

Fig. 6. Effects of cell adhesive proteins on the VEGF- or thrombin- stimulated production of Prostaglandin I_2. HUVECs were seeded at 7×10^4 cells/well on 24-well plates previously coated with Fibronectin (FN), Pronectin F (PF), Pronectin F PLUS (PFP), Retronectin (RN), or Attachin (AN). After culturing for 1 day, the cells were stimulated with 30 ng/ml of VEGF (A) or 1 U/ml of thrombin (B). One hour later, the conditioned media were collected and 6-keto $PGF_1\alpha$ concentration was determined by enzyme immunoassay. Results are expressed as picograms of $PGF_1\alpha$/ml of the supernatant and represent the mean ± S.D. of triplicate determinations. 6-Keto $PGF_1\alpha$ production from HUVECs cultured in serum-containing growing media (EGM-2) plated on a collagen-coated dish was also examined (Col/EGM).

they are expected to be put into clinical use in the near future. Serum-free culture supplemented with recombinant proteins produced without using animal-derived materials would be optimal in order to avoid contamination by animal-derived materials and transmissible agents. This work was carried out as a step in demonstrating the feasibility of recombinant cell adhesion proteins in serum-free cultures of human endothelial cells, which might form the basis of future cellular therapies. HUVECs were used as a model of tissue-derived differentiated endothelial cells.

One of the uses of endothelial cells in cellular therapy is for the vascularization of engineered tissue. Vascularization of a tissue-engineered construct is mediated primarily through the ingrowth of surrounding vessels from the peri-implant tissue. However, this process is quite slow and is not sufficient to achieve appropriate vascularization of large defects [32]. The incorporation of endothelial cells or vascular-like structure in the tissue-engineered constructs before transplantation is a possible solution of this problem. Both human embryonic stem cell-derived endothelial cells and tissue-derived endothelial cells such as HUVECs have been shown to incorporate successfully into engineered skeletal muscle tissue [33–35]. Tissue-derived human endothelial cells are also used for the endothelialization of artificial artery grafts [36]. Although serum-free media for human endothelial cells has been developed, being supplemented with a cell adhesion protein such as fibronectin is necessary [26]. Since plasma fibronectin is known to bind to several pathogens including viruses [37,38], use of a recombinant cell adhesion protein would be desired in order to avoid the contamination of infectious agents.

Another use of endothelial cells in cellular therapy is for therapeutic neovascularization, an important adaptation to rescue tissue from critical ischemia. In a rat model of myocardial infarction, transplantation of HUVECs has been shown to contribute to increased neovascularization [39]. Recently, much attention has been paid to outgrowth endothelial cells (OECs) obtained by *in vitro* culture of blood mononuclear cells [40–46]. OECs show a marked similarity to fully differentiated endothelial cells with respect to their cellular morphology, marker expression and potential to form capillary-like structures [43,44,47]. Because OECs can be obtained from blood mononuclear cells, they have the advantage that autologous endothelial cells could be obtained without invasive procedures. The potential use of OECs for therapeutic neovascularization has been shown in murine ischemia models

Please cite this article in press as: Ishii-Watabe A et al., Influences of the recombinant artificial cell adhesive proteins on the behavior of human umbilical vein endothelial cells in serum-free culture, Biologicals (2007), doi:10.1016/j.biologicals.2006.12.002

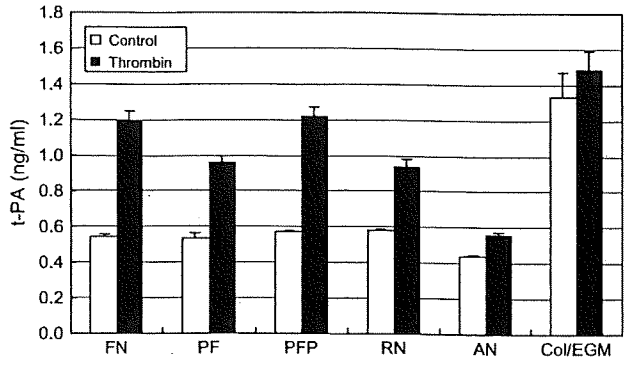

Fig. 7. Effects of cell adhesive proteins on the thrombin- stimulated production of tissue plasminogen activator. HUVECs were seeded at 7×10^4 cells/well on 24-well plates previously coated with Fibronectin (FN), Pronectin F (PF), Pronectin F PLUS (PFP), Retronectin (RN), or Attachin (AN). After culturing for 1 day, the cells were stimulated with 1 U/ml of thrombin. After 24 h incubation, the conditioned media were collected and t-PA concentration was determined by enzyme immunoassay. Results are expressed as nanograms of t-PA/ml of the supernatant and represent the mean ± S.D. of triplicate determinations. t-PA production from HUVECs cultured in serum-containing growing media (EGM-2) plated on collagen-coated dish was also examined (Col/EGM).

[47–50]. The culture conditions for OECs and for tissue-derived endothelial cells such as HUVECs are the same: endothelial basal media supplemented with fetal calf serum, VEGF, basic FGF, IGF-1, EGF and ascorbic acid. Fibronectin is the cell adhesion protein most commonly used to obtain OECs. Therefore, examining the usefulness of recombinant cell adhesion proteins as a substitute for plasma fibronectin in serum-free culture would lead to the establishment of a serum-free culture for OECs as well.

The cell culture method chosen has a direct influence on the quality and safety of cellular therapy products. The composition of media and serum are considered to affect the features of the cells, and animal-derived materials are known to carry the risk of infection or allergy. Thus, developing appropriate culture methods and ways of evaluating these methods are key to assuring the safety of cellular therapy products [11,12]. For example, when culturing human embryonic stem cells that are anticipated to be a useful source for cellular therapy products, non-human-type sialic acid (*N*-glycolyl neuraminic acid) derived from animal serum is incorporated into the sugar chain on the cell surface, which could induce an immune response

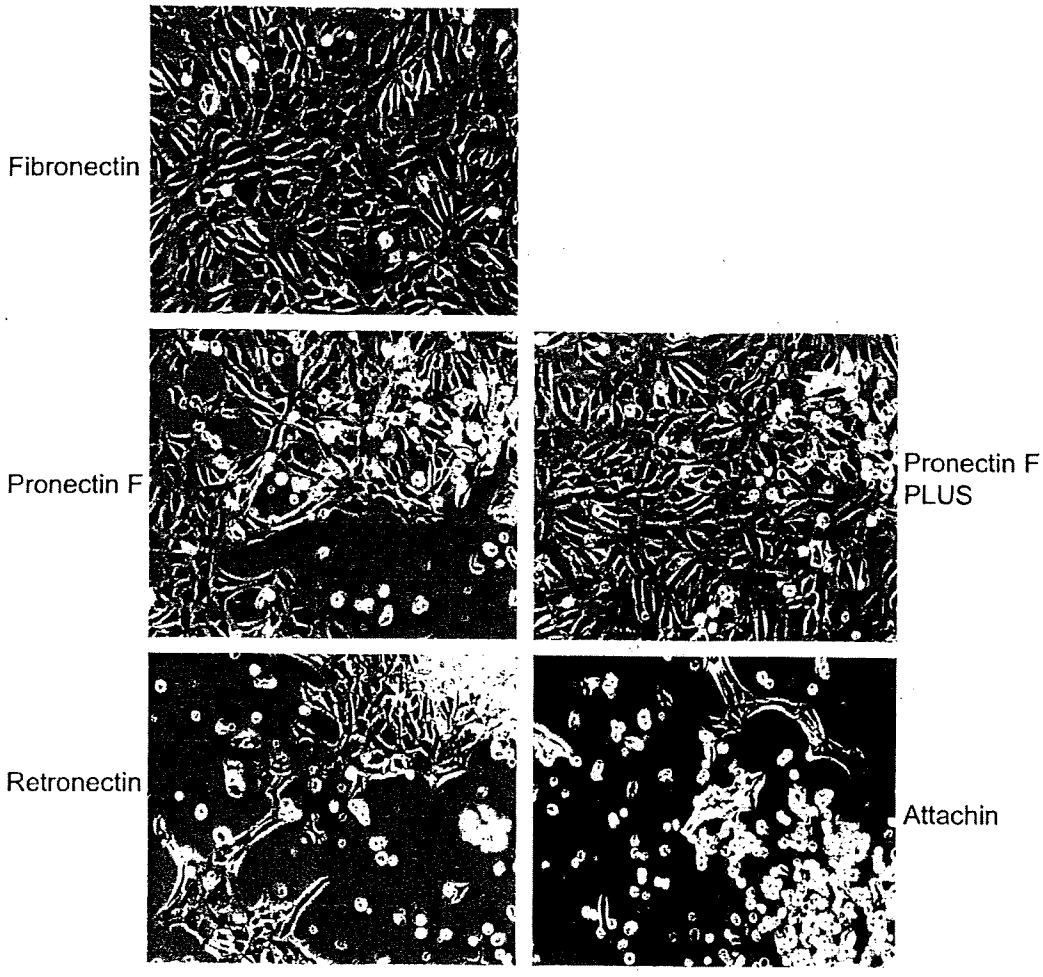

Fig. 8. Detachment of HUVECs cultured in the presence of thrombin. Cells were plated on the plates previously coated with Fibronectin, Pronectin F, Pronectin F PLUS, Retronectin, or Attachin, and cultured for 24 h in the presence of 1 U/ml of thrombin. The cells were photographed before harvesting the supernatant that is provided for the measurement of the t-PA concentration.

Please cite this article in press as: Ishii-Watabe A et al., Influences of the recombinant artificial cell adhesive proteins on the behavior of human umbilical vein endothelial cells in serum-free culture, Biologicals (2007), doi:10.1016/j.biologicals.2006.12.002

upon transplantation [51]. In addition, the transmission of unknown viruses from rodent feeder cells is also a concern [8]. Therefore, establishing cell culture methods that assure safety is an important goal in the development of cellular therapy products.

Because recombinant proteins can be produced without using animal or human-derived materials, providing the protein factors that are necessary to cell culture as recombinant proteins can contribute to improving the safety of cellular therapy products. Recombinant proteins also have an advantage in that they can provide consistent performance from lot to lot, and their function can be modified by molecular design. Artificial recombinant proteins have the possibility of being superior to naturally occurring proteins; for example, Retronectin, a deletion mutant of fibronectin that unfortunately showed less activity as an adhesive protein in this study, is much more effective in supporting gene transfer by retrovirus vectors than fibronectin [23]. If there is a concern in using artificial recombinant proteins, the residual artificial protein has the potential to show immunogenicity.

In our experiments to test cell adhesion, Pronectin F and Pronectin F PLUS were superior to fibronectin when they were used in lower concentrations (Fig. 1). This might be because both Pronectin F and Pronectin F PLUS have 13 repeats of the RGD sequence in one molecule, whereas fibronectin has only two. Pronectin F and Pronectin F PLUS are also structurally stable, and thus the coated substrates retain their performance for at least 2 years at room temperature, which is another advantage over fibronectin [52]. Pronectins were produced without using any animal-derived components (Dr. Kurokawa, Sanyo Kasei Kogyo, personal communication).

Pronectin F is not soluble in water since the silk-like protein sequence forms strong hydrogen bonds intermolecularly; thus, it must be dissolved in $LiClO_4$ [21]. Therefore, Pronectin F PLUS, a water-soluble variant of Pronectin F, was developed by chemical modification of the serine residues of Pronectin F [22]. As shown in Fig. 3, a higher amount of Pronectin F was absorbed on polystyrene dishes than Pronectin F PLUS. Since the surface of polystyrene plates is hydrophobic, hydrophobic Pronectin F might have been absorbed well. Pronectin L, which has a similar core sequence to that of Pronectin F, was also absorbed well on the dish, although no cells adhered on it.

In spite of their differences in absorption on the polystyrene dish, Pronectin F PLUS and Pronectin F showed similar efficiency with respect to the adhered cell number, growth support, induction of FAK phosphorylation, and production of PGI_2 and t-PA. Moreover, Pronectin F PLUS was more potent than Pronectin F in its support of cell adhesion under stimulation with thrombin (Fig. 9). The cells on Pronectin F PLUS were resistant to cell detachment due to the thrombin-induced cytoskeletal changes. This might be because that Pronectin F PLUS is positively charged by chemical modification. Since the cell surface possesses a negative charge, the adhesive intensity between the cells and Pronectin F PLUS was increased due to the static electrical interaction, resulting in the maintenance of cell adhesiveness after the cytoskeletal change

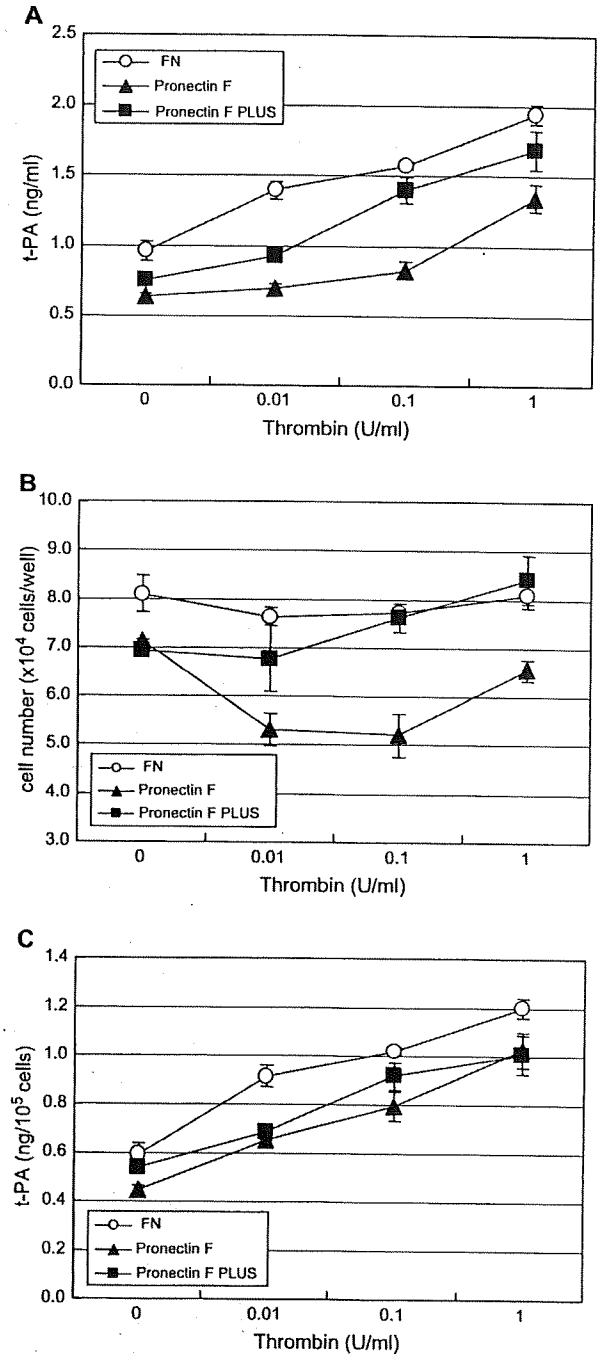

Fig. 9. Thrombin-induced production of t-PA and decrease in viability of HUVECs adhered on Pronectin F. HUVECs were seeded at 7×10^4 cells/well on 24-well plates previously coated with Fibronectin, Pronectin F or Pronectin F PLUS. After culturing for 1 day, the cells were stimulated with thrombin at the indicated concentrations. After 24 h incubation, the conditioned media were collected and t-PA concentration was determined by enzyme immunoassay (A). The cell numbers were determined using a Cell-Counting Kit-8 (B). Production of t-PA per 10^5 cells was calculated (C). Each data point represents the mean ± S.D. of triplicate determinations.

Please cite this article in press as: Ishii-Watabe A et al., Influences of the recombinant artificial cell adhesive proteins on the behavior of human umbilical vein endothelial cells in serum-free culture, Biologicals (2007), doi:10.1016/j.biologicals.2006.12.002

induced by thrombin. To our knowledge, this is the first observation to reveal the difference in biological properties between Pronectin F and Pronectin F PLUS. The retention of human endothelial cells on the lumen in the presence of physiological stimuli is an important prerequisite for artificial artery grafts to be successful, and, therefore, Pronectin F PLUS could also be suited for use in this type of graft.

In the present study, the usefulness of Pronectin F PLUS as a substitute for fibronectin was indicated; however, Pronectin F PLUS and Pronectin F were less effective than fibronectin in long-term cell cultures. We were able to culture HUVECs up to around 6 passages using the serum-free media with fibronectin. However, when Pronectin F or Pronectin F PLUS was used instead of fibronectin, the cell number did not increase beyond the second passage. Although Pronectin F PLUS worked better than Pronectin F, the efficiency of both was lower than that of fibronectin in the long-term maintenance of HUVECs. Since fibronectin has several functional domains that can bind to heparin, fibrin and collagen, signals other than the RGD-integrin interaction would be important in the long-term maintenance of the cells. The incorporation of domains other than that of RGD of fibronectin into Pronectin F PLUS would be necessary to improve its efficacy in long-term cell cultures.

For cell cultures, porcine trypsin is often used when cells are harvested. The use of trypsin may lead to the contamination of animal-derived materials or transmissible agents. In serum-free cultures of HUVECs, we were able to harvest cells for passage using a protease free of animal-derived materials such as TrypLE Select (Invitrogen, Carlsbad, CA, USA) or AccuMax (Chemicon, Billerica, MA, USA); therefore, trypsin is not necessarily used for the maintenance of HUVECs, which means that it is possible to eliminate the potential for contamination of animal-derived proteins.

In summary, Pronectin F PLUS was shown to have the closest activity to plasma fibronectin in the serum-free culture of HUVECs by examining VEGF- or bFGF-induced cell proliferation, FAK phosphorylation, and thrombin-stimulated production of PGI_2 or t-PA. The cell adherent activity of Pronectin F PLUS was superior to fibronectin at concentrations of less than 1 μg/ml. Although Pronectin F PLUS has the same amino acid sequence as Pronectin F, only HUVECs on Pronectin F PLUS were resistant to thrombin-induced cell detachment. Pronectin F PLUS is thus thought to be a promising substitute for plasma fibronectin in the serum-free culture of endothelial cells, although modification would be necessary to improve its efficiency in long-term cell cultures.

Acknowledgements

This work was supported in part by a Grant-in-Aid for Health and Labor Science Research (H17-SAISEI-021 and H17-IYAKU-015) from the Japanese Ministry of Health, Labor and Welfare, and a Grant-in-Aid for Young Scientists (B) from the Ministry of Education, Science, Sports and Culture.

References

[1] Wollert KC, Drexler H. Cell-based therapy for heart failure. Curr Opin Cardiol 2006;21:234–9.
[2] Zavos PM. Stem cells and cellular therapy: potential treatment for cardiovascular diseases. Int J Cardiol 2006;107:1–6.
[3] Fazel S, Tang GH, Angoulvant D, Cimini M, Weisel RD, Li RK, et al. Current status of cellular therapy for ischemic heart disease. Ann Thorac Surg 2005;79:S2238–47.
[4] http://www.fda.gov/cber/gdlns/somgene.pdf.
[5] http://www.fda.gov/cber/gdlns/cmcsomcell.pdf.
[6] http://www.emea.eu.int/pdfs/human/cpwp/32377405en.pdf.
[7] http://www.fda.gov/cber/rules/suitdonor.pdf.
[8] Lee JB, Lee JE, Park JH, Kim SJ, Kim MK, Roh SI, et al. Establishment and maintenance of human embryonic stem cell lines on human feeder cells derived from uterine endometrium under serum-free condition. Biol Reprod 2005;72:42–9.
[9] Ogawa K, Matsui H, Ohtsuka S, Niwa H. A novel mechanism for regulating clonal propagation of mouse ES cells. Genes Cells 2004;9:471–7.
[10] Asher DM. Bovine sera used in the manufacture of biologicals: current concerns and policies of the U.S. Food and Drug Administration regarding the transmissible spongiform encephalopathies. Dev Biol Stand 1999; 99:41–4.
[11] Asher DM. The transmissible spongiform encephalopathy agents: concerns and responses of United States regulatory agencies in maintaining the safety of biologics. Dev Biol Stand 1999;100:103–18.
[12] Cobo F, Stacey GN, Hunt C, Cabrera C, Nieto A, Montes R, et al. Microbiological control in stem cell banks: approaches to standardisation. Appl Microbiol Biotechnol 2005;68:456–66.
[13] Cobo F, Talavera P, Concha A. Diagnostic approaches for viruses and prions in stem cell banks. Virology 2006;347:1–10.
[14] Kornblihtt AR, Umezawa K, Vibe-Pedersen K, Baralle FE. Primary structure of human fibronectin: differential splicing may generate at least 10 polypeptides from a single gene. EMBO J 1985;4:1755–9.
[15] Umezawa K, Kornblihtt AR, Baralle FE. Isolation and characterization of cDNA clones for human liver fibronectin. FEBS Lett 1985;186:31–4.
[16] Pierschbacher MD, Ruoslahti E. Cell attachment activity of fibronectin can be duplicated by small synthetic fragments of the molecule. Nature 1984;309:30–3.
[17] Ruoslahti E, Pierschbacher MD. New perspectives in cell adhesion: RGD and integrins. Science 1987;238:491–7.
[18] Bourdoulous S, Orend G, MacKenna DA, Pasqualini R, Ruoslahti E. Fibronectin matrix regulates activation of RHO and CDC42 GTPases and cell cycle progression. J Cell Biol 1998;143:267–76.
[19] Frisch SM, Ruoslahti E. Integrins and anoikis. Curr Opin Cell Biol 1997;9:701–6.
[20] Heslot H. Artificial fibrous proteins: a review. Biochimie 1998;80:19–31.
[21] Cappello J. Genetically Engineered Protein Polymers. In: Domb AJ, Kost J, Wiseman D, editors. Handbook of Biodegradable Polymers. Amsterdam: Harwood Academic Publishers; 1997. p. 387–416.
[22] Hosseinkhani H, Tabata Y. PEGylation enhances tumor targeting of plasmid DNA by an artificial cationized protein with repeated RGD sequences, Pronectin. J Control Release 2004;97:157–71.
[23] Hanenberg H, Xiao XL, Dilloo D, Hashino K, Kato I, Williams DA. Colocalization of retrovirus and target cells on specific fibronectin fragments increases genetic transduction of mammalian cells. Nat Med 1996;2:876–82.
[24] http://home.kimo.com.tw/biotaichchen/Attachin/into.html.
[25] http://home.kimo.com.tw/biotaichchen/Attachin/qa.html.
[26] Gorfien S, Spector A, DeLuca D, Weiss S. Growth and physiological functions of vascular endothelial cells in a new serum-free medium (SFM). Exp Cell Res 1993;206:291–301.
[27] Zaric J, Ruegg C. Integrin-mediated adhesion and soluble ligand binding stabilize COX-2 protein levels in endothelial cells by inducing expression and preventing degradation. J Biol Chem 2005;280:1077–85.
[28] Ilic D, Kovacic B, Johkura K, Schlaepfer DD, Tomasevic N, Han Q, et al. FAK promotes organization of fibronectin matrix and fibrillar adhesions. J Cell Sci 2004;117:177–87.

Please cite this article in press as: Ishii-Watabe A et al., Influences of the recombinant artificial cell adhesive proteins on the behavior of human umbilical vein endothelial cells in serum-free culture, Biologicals (2007), doi:10.1016/j.biologicals.2006.12.002

[29] Almeida EA, Ilic D, Han Q, Hauck CR, Jin F, Kawakatsu H, et al. Matrix survival signaling: from fibronectin via focal adhesion kinase to c-Jun NH(2)-terminal kinase. J Cell Biol 2000;149:741–54.
[30] Schlaepfer DD, Broome MA, Hunter T. Fibronectin-stimulated signaling from a focal adhesion kinase-c-Src complex: involvement of the Grb2, p130cas, and Nck adaptor proteins. Mol Cell Biol 1997;17:1702–13.
[31] Ruest PJ, Roy S, Shi E, Mernaugh RL, Hanks SK. Phosphospecific antibodies reveal focal adhesion kinase activation loop phosphorylation in nascent and mature focal adhesions and requirement for the autophosphorylation site. Cell Growth Differ 2000;11:41–8.
[32] Fuchs S, Motta A, Migliaresi C, Kirkpatrick CJ. Outgrowth endothelial cells isolated and expanded from human peripheral blood progenitor cells as a potential source of autologous cells for endothelialization of silk fibroin biomaterials. Biomaterials 2006;27:5399–408.
[33] Jain RK, Au P, Tam J, Duda DG, Fukumura D. Engineering vascularized tissue. Nat Biotechnol 2005;23:821–3.
[34] Levenberg S, Rouwkema J, Macdonald M, Garfein ES, Kohane DS, Darland DC, et al. Engineering vascularized skeletal muscle tissue. Nat Biotechnol 2005;23:879–84.
[35] Koike N, Fukumura D, Gralla O, Au P, Schechner JS, Jain RK. Tissue engineering: creation of long-lasting blood vessels. Nature 2004;428:138–9.
[36] Meinhart JG, Schense JC, Schima H, Gorlitzer M, Hubbell JA, Deutsch M, et al. Enhanced endothelial cell retention on shear-stressed synthetic vascular grafts precoated with RGD-cross-linked fibrin. Tissue Eng 2005;11:887–95.
[37] Julkunen I, Hautanen A, Keski-Oja J. Interaction of viral envelope glycoproteins with fibronectin. Infect Immun 1983;40:876–81.
[38] Torre D, Pugliese A, Ferrario G, Marietti G, Forno B, Zeroli C. Interaction of human plasma fibronectin with viral proteins of human immunodeficiency virus. FEMS Immunol Med Microbiol 1994;8:127–31.
[39] Merx MW, Zernecke A, Liehn EA, Schuh A, Skobel E, Butzbach B, et al. Transplantation of human umbilical vein endothelial cells improves left ventricular function in a rat model of myocardial infarction. Basic Res Cardiol 2005;100:208–16.
[40] Fuchs S, Hermanns MI, Kirkpatrick CJ. Retention of a differentiated endothelial phenotype by outgrowth endothelial cells isolated from human peripheral blood and expanded in long-term cultures. Cell Tissue Res 2006;326:79–92.
[41] Cai H, Gehrig P, Scott TM, Zimmermann R, Schlapbach R, Zisch AH. MnSOD marks cord blood late outgrowth endothelial cells and accompanies robust resistance to oxidative stress. Biochem Biophys Res Commun 2006;350:364–9.
[42] Sharpe 3rd EE, Teleron AA, Li B, Price J, Sands MS, Alford K, et al. The origin and in vivo significance of murine and human culture-expanded endothelial progenitor cells. Am J Pathol 2006;168:1710–21.
[43] Gulati R, Jevremovic D, Peterson TE, Chatterjee S, Shah V, Vile RG, et al. Diverse origin and function of cells with endothelial phenotype obtained from adult human blood. Circ Res 2003;93:1023–5.
[44] Lin Y, Weisdorf DJ, Solovey A, Hebbel RP. Origins of circulating endothelial cells and endothelial outgrowth from blood. J Clin Invest 2000; 105:71–7.
[45] Smadja DM, Bieche I, Uzan G, Bompais H, Muller L, Boisson-Vidal C, et al. PAR-1 activation on human late endothelial progenitor cells enhances angiogenesis in vitro with upregulation of the SDF-1/CXCR4 system. Arterioscler Thromb Vasc Biol 2005;25:2321–7.
[46] Eggermann J, Kliche S, Jarmy G, Hoffmann K, Mayr-Beyrle U, Debatin KM, et al. Endothelial progenitor cell culture and differentiation in vitro: a methodological comparison using human umbilical cord blood. Cardiovasc Res 2003;58:478–86.
[47] Hur J, Yoon CH, Kim HS, Choi JH, Kang HJ, Hwang KK, et al. Characterization of two types of endothelial progenitor cells and their different contributions to neovasculogenesis. Arterioscler Thromb Vasc Biol 2004;24:288–93.
[48] Yoon CH, Hur J, Park KW, Kim JH, Lee CS, Oh IY, et al. Synergistic neovascularization by mixed transplantation of early endothelial progenitor cells and late outgrowth endothelial cells: the role of angiogenic cytokines and matrix metalloproteinases. Circulation 2005;112: 1618–27.
[49] Ott I, Keller U, Knoedler M, Gotze KS, Doss K, Fischer P, et al. Endothelial-like cells expanded from CD34+ blood cells improve left ventricular function after experimental myocardial infarction. FASEB J 2005; 19:992–4.
[50] Choi JH, Hur J, Yoon CH, Kim JH, Lee CS, Youn SW, et al. Augmentation of therapeutic angiogenesis using genetically modified human endothelial progenitor cells with altered glycogen synthase kinase-3beta activity. J Biol Chem 2004;279:49430–8.
[51] Martin MJ, Muotri A, Gage F, Varki A. Human embryonic stem cells express an immunogenic nonhuman sialic acid. Nat Med 2005;11: 228–32.
[52] http://www.sanyo-chemical.co.jp/product/pronectin/eng/prodspec.htm.

Please cite this article in press as: Ishii-Watabe A et al., Influences of the recombinant artificial cell adhesive proteins on the behavior of human umbilical vein endothelial cells in serum-free culture, Biologicals (2007), doi:10.1016/j.biologicals.2006.12.002

Pharmaceutical Research, Vol. 24, No. 9, September 2007 (© 2007)
DOI: 10.1007/s11095-007-9296-2

Research Paper

Significance of Local Mobility in Aggregation of β-Galactosidase Lyophilized with Trehalose, Sucrose or Stachyose

Sumie Yoshioka,[1,2] Tamaki Miyazaki,[1] Yukio Aso,[1] and Tohru Kawanishi[1]

Received January 3, 2007; accepted March 14, 2007; published online April 3, 2007

Purpose. The purpose of this study is to compare the effects of global mobility, as reflected by glass transition temperature (T_g) and local mobility, as reflected by rotating-frame spin-lattice relaxation time ($T_{1\rho}$) on aggregation during storage of lyophilized β-galactosidase (β-GA).
Materials and Methods. The storage stability of β-GA lyophilized with sucrose, trehalose or stachyose was investigated at 12% relative humidity and various temperatures (40–90°C). β-GA aggregation was monitored by size exclusion chromatography (SEC). Furthermore, the $T_{1\rho}$ of the β-GA carbonyl carbon was measured by ^{13}C solid-state NMR, and T_g was measured by modulated temperature differential scanning calorimetry. Changes in protein structure during freeze drying were measured by solid-state FT-IR.
Results. The aggregation rate of β-GA in lyophilized formulations exhibited a change in slope at around T_g, indicating the effect of molecular mobility on the aggregation rate. Although the T_g rank order of β-GA formulations was sucrose < trehalose < stachyose, the rank order of β-GA aggregation rate at temperatures below and above T_g was also sucrose < trehalose < stachyose, thus suggesting that β-GA aggregation rate is not related to ($T-T_g$). The local mobility of β-GA, as determined by the $T_{1\rho}$ of the β-GA carbonyl carbon, was more markedly decreased by the addition of sucrose than by the addition of stachyose. The effect of trehalose on $T_{1\rho}$ was intermediate when compared to those for sucrose and stachyose. These findings suggest that β-GA aggregation rate is primarily related to local mobility. Significant differences in the second derivative FT-IR spectra were not observed between the excipients, and the differences in β-GA aggregation rate observed between the excipients could not be attributed to differences in protein secondary structure.
Conclusions. The aggregation rate of β-GA in lyophilized formulations unexpectedly correlated with the local mobility of β-GA, as indicated by $T_{1\rho}$, rather than with ($T-T_g$). Sucrose exhibited the most intense stabilizing effect due to the most intense ability to inhibit local protein mobility during storage.

KEY WORDS: β-galactosidase; global mobility; local mobility; lyophilized formulation; solid-state stability.

INTRODUCTION

Close correlations between storage stability and molecular mobility have been demonstrated for various lyophilized formulations of peptides and proteins (1,2). Aggregation between protein molecules is a degradation pathway commonly observed in lyophilized protein formulations. The rate of protein aggregation is generally considered to depend on the translational mobility of protein molecules, which is related to structural relaxation (α-relaxation) of the formulation. Correlations between aggregation rates and structural relaxation have been shown in various protein systems in visible ways, such as enhancement of aggregation associated with decreases in glass transition temperature (T_g) (3–6) and changes in the temperature dependence of aggregation rates around T_g (7–10). However, recent studies have suggested that molecular mobility with a length scale shorter than structural relaxation (β-relaxation or local mobility), rather than structural relaxation, is critical to protein aggregation (11,12).

The rate of protein aggregation in lyophilized formulations is also affected by the degree of change in protein conformation produced during the freeze-drying process (1). Greater changes in protein conformation are considered to lead to enhanced aggregation during subsequent storage.

In this study, the significance of local mobility in aggregation of lyophilized β-galactosidase (β-GA), a model protein, is discussed in comparison with the significance of structural relaxation and conformational changes. β-GA underwent significant inactivation during freeze drying with dextran, thus suggesting that significant conformational changes occurred during the process (13). When freeze dried with polyvinylalcohol or methylcellulose, inactivation was not observed during freeze drying (10). However, the time

[1] Division of Drugs, National Institute of Health Sciences, 1-18-1 Kamiyoga, Setagaya-ku, Tokyo 158-8501, Japan.
[2] To whom correspondence should be addressed. (e-mail: yoshioka@nihs.go.jp)

0724-8741/07/0900-1660/0

courses of aggregation during subsequent storage were describable with the empirical Kohlrausch-Williams-Watts (KWW) equation, thus leading to speculation that there were protein molecules having different conformations resulting from stresses during the freeze-drying process, each aggregating with a different time constant (10,14). The temperature dependence of the aggregation rate measured at the initial stage changed around T_{mc} (T_g determined by NMR relaxation measurement (15)), showing an apparent correlation between aggregation rate and structural relaxation (10). In this study, the significance of local obility in aggregation of lyophilized β-GA was examined in comparison with that of structural relaxation. The aggregation rates of β-GA lyophilized with trehalose, sucrose or stachyose were measured at temperatures near T_g, and correlations were examined between aggregation rate and local mobility (as measured by solid-state NMR), T_g (a primary parameter of structural relaxation), or protein conformational changes (as measured by FT-IR).

MATERIALS AND METHODS

Preparation of Lyophilized β-GA Formulations

β-GA from Aspergillus oryzae (10 U/mg; molecular weight: 105,000; isoelectric point:4.6) was kindly provided by Amano Enzyme Inc. (Nagoya, Japan) and purified by dialysis against 2.5 mM sodium phosphate solution of pH 4.5 (adjusted with HCl). After concentrated by ultrafiltration, trehalose (203-02252, Wako Pure Chemical Ind. Ltd, Osaka, Japan), sucrose (S-9378, Sigma Chemical Co., St. Louis, MO, USA) or stachyose (S-4001, Sigma Chemical Co., St. Louis, MO, USA) solution was added to make a 3.3 mg/ml β-GA solution with various weight fractions of excipient. Two hundred microliters of the solution was frozen in a polypropylene sample tube (2.0 ml) by immersion in liquid nitrogen for 10 min, and then dried at a vacuum level below 5 Pa for 23.5 h in a lyophilizer (Freezevac C-1, Tozai Tsusho Co., Tokyo, Japan). The shelf temperature was between −35 and −30°C for the first 10 h, 20°C for the subsequent 10 h, and 30°C for the last 3.5 h.

Determination of Water Sorption and T_g of Lyophilized β-GA Formulations

Water vapor absorption isotherms were measured gravimetrically at 25°C for lyophilized β-GA formulations containing trehalose, sucrose or stachyose using the automated sorption analyzer (MB-300 G system, VTI Corp., FL, USA). Samples were dried at 25°C under a vacuum level below 0.1 Pa until changes in weight were less than 1 μg per 10 min. Water contents of the samples at partial vapor pressures of 0.10 and 0.20 (corresponding to 10 and 20% relative humidity (RH), respectively) were determined based on equilibrated sample weight (changes in weight of less than 1 μg per 10 min).

The T_g of lyophilized β-GA formulations was determined by modulated temperature differential scanning calorimetry (2920; TA Instruments, DE, USA). Before T_g measurements, samples were stored at 15°C for 24 h in a desiccator with a saturated solution of LiCl H_2O (12% RH). The conditions were as follows: modulation period of 100 s, a modulation amplitude of ±0.5°C, and an underlying heating rate of 1°C/min. Samples were put in a hermetic pan. Temperature calibration was performed using indium.

Determination of $T_{1\rho}$ of β-GA Carbonyl Carbon by ^{13}C Solid-state NMR

The rotating-frame spin-lattice relaxation time ($T_{1\rho}$) of β-GA carbonyl carbon in lyophilized formulations containing various weight fractions of trehalose, sucrose and stachyose was determined at 25°C using a UNITY plus spectrometer operating at a proton resonance frequency of 400 MHz (Varian Inc., CA, USA). Lyophilized samples were pre-equilibrated at 12% RH. Spin-locking field was equivalent to 19 kHz. The rotor size was 7 mm and spinning speed was 4 kHz. Peak height at approximately 180 ppm due to β-GA carbonyl carbon was followed with delay times of 1, 5, 10, 20, 30, 50 and 80 ms. Similar measurement of $T_{1\rho}$ was performed for lyophilized β-GA alone.

Fourier Transform Infra Red (FT-IR) Spectroscopy Measurements

FT-IR spectroscopy was performed using a JASCO FT/IR-6300 spectrometer (JASCO, Tokyo, Japan). A mixture of 100 mg KBr and 1–2 mg lyophilized β-GA formulation was pressed into a pellet under vacuum. A total of 256 scans and a resolution of 4 cm^{-1} were used for each spectrum. The second-derivative spectra were obtained from intact spectra without smoothing using Spectra Manager software version 2 (JASCO, Tokyo, Japan). The area of spectral absorbance was calculated using a baseline drawn between 1,600 and 1,700 cm^{-1}, and normalized for comparison between the formulations containing different excipients.

Determination of β-GA Aggregation Rate in Lyophilized Formulations

Lyophilized β-GA formulations containing trehalose, sucrose or stachyose, pre-equilibrated at 12% RH, were stored with a tight screw-cap at a constant temperature (40–90°C), removed at various times, and stored in liquid nitrogen until assayed. Samples were reconstituted in 1.7 ml of 200 mM phosphate buffer (pH 6.2), and injected into a size exclusion chromatography as described previously (10). The column (Tosoh G3000SW, 30 cm×7.5 mm, Tokyo) was maintained at 30°C, and 200 mM phosphate buffer (pH 6.2) was used as the mobile phase. The detection wavelength was 280 nm. Monomeric β-GA was determined based on the peak height of its chromatogram.

Reconstitution of lyophilized β-GA formulations after storage was also carried out using reconstitution mediums of 200 mM phosphate buffer (pH 6.2) containing 0.5% additives (dextran sulfate (197-08362, Wako Pure Chemical Ind. Ltd, Osaka, Japan), 2-hydroxylpropyl-β-cyclodextrin (C-0926, Sigma Chemical Co.), poly-L-lysine (P-7890, Sigma Chemical Co.), or pluronic (F-68, P-7061, Sigma Chemical Co., St. Louis, MO, USA).

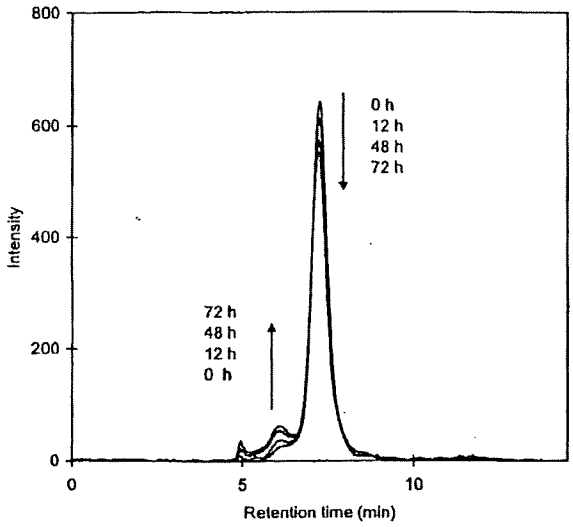

Fig. 1. Size-exclusion chromatograms of β-GA lyophilized with trehalose after various periods of storage at 80°C and 12%RH. The weight fraction of trehalose : 0.5.

RESULTS AND DISCUSSION

Aggregation of β-GA during Storage of Lyophilized Formulations

Figure 1 shows representative size-exclusion chromatograms of β-GA in lyophilized formulations, indicating that monomeric β-GA aggregates to larger sizes during storage. Tables I and II show the effects of reconstitution medium on the amount of monomeric β-GA remaining after storage of the formulation containing trehalose at temperatures below and above T_g, respectively. The amount of monomeric β-GA was not significantly affected by the addition of dextran sulfate or poly-L-lysine. Addition of pluronic also had no significant effect on the amount of monomeric β-GA. For lyophilized interleukin-2, the amount of aggregates after reconstitution was decreased by addition of poly-ions with high charge density, such as dextran sulfate and poly-L-lysine, and increased by addition of surfactants, such as pluronic, into the reconstitution buffer solution (16). This may be explained by assuming that the formation of aggregates from partially unfolded intermediates, as well as the reverse formation of native protein from intermediates, occur during the reconstitution process. In contrast, the lack of the effects of additives observed for β-GA aggregation indicates that neither formation of aggregates nor reverse formation of native protein from partially unfolded intermediates occurs during the reconstitution process. This finding suggests that β-GA aggregation occurs during the storage of lyophilized formulations, even at temperatures below T_g. Because large-scale diffusion of protein molecules is considered to be very limited in glassy solids, β-GA aggregation is considered to occur between protein molecules that are adjacent to each other without large-scale diffusion.

Temperature Dependence of β-GA Aggregation Rate

Figure 2 shows time courses of aggregation of β-GA at 50°C (below T_g) for lyophilized formulations with an excipient fraction of 0.33, and at 80°C (above T_g) for lyophilized formulations with an excipient fraction of 0.5. Similar time courses were obtained for formulations with various excipient fractions and at various temperatures. The wide range of the time courses could be better described by the KWW equation, but the initial stages of aggregation were describable with first-order kinetics. The solid line in Fig. 2 represents the theoretical time course of first-order kinetics.

The time required for 10% degradation (t_{90}) was calculated from the apparent first-order rate constant. Figure 3 shows the temperature-dependence of t_{90} determined for aggregation of β-GA lyophilized with sucrose, trehalose or stachyose at an excipient fractions of 0.33 and 0.5, 12% RH and various temperatures. For the sucrose and trehalose formulations, the temperature dependence of t_{90} exhibited a change in the slope at around T_g, suggesting significant effects of molecular mobility. For the stachyose formulation, the change in the slope was not obvious, because few data were available at temperatures above T_g. The values of t_{90} at T_g largely depended on the excipient; sucrose > trehalose > stachyose. The finding that the t_{90} values at T_g varied significantly between these three formulations suggests that β-GA aggregation rate is not primarily related to $(T-T_g)$.

Table I. Effects of Reconstitution Medium on β-GA Aggregation Below T_g for 0.09 Trehalose Formulation

Additives in Reconstitution Medium	Peak Height for Monomeric β-GA (Relative to Solution Prior to Freeze Drying)			
	After Freeze Drying		After 24 h-storage at 70°C	
None	0.97	(0.01)	0.65	(0.01)
Dextran Sulfate	0.96	(0.00)	0.62	(0.01)
2-hydroxylpropyl-β-cyclodextrin	0.95	(0.01)	0.62	(0.00)
Poly-L-lysine	0.94	(0.01)	0.62	(0.00)
Pluronic	0.97	(0.01)	0.66	(0.01)

0.5% additives
Values in brackets represent standard deviation (n=3)